

Orotidine-5'-Monophosphate Decarboxylase:

Purification and Spectral Studies

by

Lana Y. Saleh

Submitted in Partial Fulfillment of the Requirements

for the Degree of

Masters of Science

in the

Chemistry

Program

YOUNGSTOWN STATE UNIVERSITY

August, 1999


## Orotidine-5'-Monophosphate Decarboxylase:

## Purification and Spectral Studies

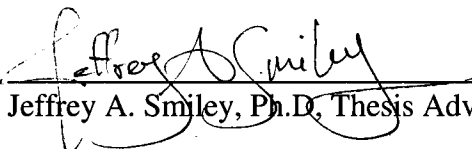
Lana Y. Saleh

I hereby release this thesis to the public. I understand this thesis will be housed at the Circulation Desk of the University Library and will be available for public access. I also authorize the university of other individuals to make copies of this thesis as needed for scholarly research.

Signature:

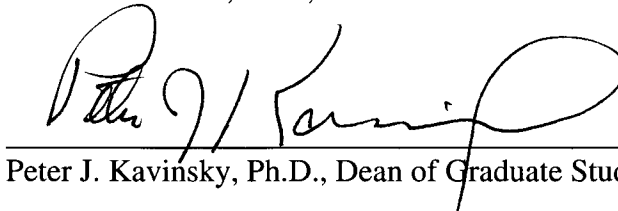
  
Lana Y. Saleh 8/17/99  
Date

Approvals:

  
Jeffrey A. Smiley, Ph.D., Thesis Advisor 8/17/99  
Date

  
John A. Jackson, Ph.D., Committee Member 8/17/99  
Date

  
Michael A. Serra, Ph.D., Committee Member 8/17/99  
Date

  
Peter J. Kavinsky, Ph.D., Dean of Graduate Studies 8/18/99  
Date

## Abstract

The chemical mechanism by which orotidylate decarboxylase (ODCase) catalyzes the formation of uridylate (UMP) from orotidylate (OMP) is apparently different from any of the common decarboxylation routes seen with other enzymes. ODCase is the final enzyme of the *de novo* pyrimidine biosynthetic pathway and it displays one of the largest rate enhancements ever measured. Different mechanisms have been suggested to explain the mechanistic action of ODCase. Our group suggested a model for this decarboxylation that involves proton donation to the transition state in a concerted protonation/decarboxylation mechanism and possible participation of a  $Zn^{+2}$  ion. Yeast ODCase was purified from any contaminating proteins whereas its mutant (K93C) was partially purified. Thio-substituted analogues were used as inhibitors to probe the active site of the enzyme. The inhibition constants of these compounds were measured by  $^{14}CO_2$  displacement assays, and their  $pK_a$ 's were determined by spectrophotometric assays.  $^1H$  NMR spectroscopy of ODCase in complex with barbituric acid ribonucleotide (BMP) at different  $D_2O$  concentrations and UMP at 10%  $D_2O$  reveals downfield signals, possibly identifying hydrogen bonds between the enzyme and the inhibitor. The two farthest downfield signals in the spectra are absent in the free ODCase spectrum. Our proposed catalytic mechanism and the results obtained from the experiments are to be discussed in this thesis.

## Acknowledgements

I wish to express my gratitude and love to my parents and sisters who supported me through all these years; without them I could not have achieved my goals. I also appreciate the great hospitality and love that my uncle Ayman and his family showed in the past two years. Likewise, I would like to thank my uncle Hussain, uncle Maher, and their families for their support and understanding. My warmest wishes go to Danny, Scott, Shelly, Carolyn, Rob, Julie, Greg, and Chris with whom I spent the best time in these two years.

I would also like to thank my advisor Dr. Jeffrey Smiley for his guidance and help in the lab. My recognition goes to Dr. John Jackson and Michael Serra who reviewed this thesis with patience and understanding. My admiration goes to Dr. Janet Delbene who is the best physical chemistry professor I have had. I would also like to thank Dr. Peter Norris for answering all my organic questions. Finally, I would like to thank the Department of Chemistry at Youngstown State University for giving me the opportunity to pursue a Master's degree.

## Table of Contents

Title Page .....	i
Signature Page.....	ii
Abstract .....	iii
Acknowledgements .....	iv
Table of Contents .....	v-vi
List of Figures .....	vii-viii
List of Tables.....	ix
List of Symbols and Abbreviations.....	x-xi
<b>Chapter 1 Introduction</b>	
Introduction .....	1-6
ODCase: Historical Background.....	7-13
The Low Barrier Hydrogen Bond .....	13-14
<b>Chapter 2 Yeast ODCase Purification and Stabilization</b>	
Introduction .....	15-16
Affinity Chromatography.....	16-17
Ion Exchange Chromatography.....	17-18
SDS-Polyacrylamide Gel Electrophoresis .....	18
The Bradford Assay .....	18-19
Materials.....	19
Yeast Growth Protocol .....	19-20
Purification of Yeast ODCase .....	20-22
<b>Chapter 3 Inhibition Constants of ODCase Ligands</b>	
Introduction .....	31-32
Materials.....	32

**Table of Contents (Continued)**

2-ThioUMP Synthesis .....	32-33
UPRTase Preparation .....	32
Synthesis of 2-ThioUMP .....	32-33
Ionization Constants of Thio-Substituted Analogues .....	33-34
Enzyme Assays .....	34-37
4-ThioUMP .....	34-35
2-ThioUMP .....	35-37
Discussion .....	37-39
 Chapter 4 <sup>1</sup> H NMR Spectral Studies of ODCase Complexes	
Introduction .....	48
Materials .....	48
Methods .....	48-49
Results and Discussion .....	49-50
Conclusion .....	53-54
References .....	55-56

**List of Figures**

<b>Figure 1</b>	Enolate Intermediate in Decarboxylation .....	1
<b>Figure 2</b>	Catalytic Mechanism of Oxaloacetate Decarboxylase .....	2
<b>Figure 3</b>	Decarboxylation of 6-Phosphogluconic Acid.....	3
<b>Figure 4</b>	Amino Acid Decarboxylases with Pyridoxal Phosphate .....	4
<b>Figure 5</b>	Conformation and Stereochemistry of Decarboxylation .....	5
<b>Figure 6</b>	Mechanism of Decarboxylation of Pyruvate .....	6
<b>Figure 7</b>	ODCase Reaction.....	7
<b>Figure 8</b>	pGU2 Plasmid.....	8
<b>Figure 9</b>	Lee and Houk's ODCase Mechanism.....	9
<b>Figure 10</b>	Zwitterion/Ylide Mechanism for ODCase.....	10
<b>Figure 11</b>	Beak and Siegel's Addition-Elimination Mechanism .....	11
<b>Figure 12</b>	Cibacron Blue Coupled to Agarose .....	17
<b>Figure 13</b>	Affi-Gel Blue Purified Wild Type ODCase on SDS-PAGE .....	23
<b>Figure 14</b>	FPLC Purified Wild Type ODCase on SDS-PAGE .....	23
<b>Figure 15</b>	FPLC Pooled Wild Type ODCase on SDS-PAGE.....	24
<b>Figure 16</b>	Affi-Gel Blue Purified Wild Type ODCase on SDS-PAGE .....	24
<b>Figure 17</b>	Affi-Gel Blue Purified Mutant ODCase on SDS-PAGE .....	25
<b>Figure 18</b>	FPLC Pooled Mutant ODCase on SDS-PAGE.....	25
<b>Figure 19</b>	Bradford Assay Curve .....	30
<b>Figure 20</b>	Thio-Substituted Analogues .....	32
<b>Figure 21</b>	Theoretical Titration Curve .....	44
<b>Figure 22</b>	Titration Curve of 4-ThioUMP .....	45

**List of Figures (Continued)**

<b>Figure 23</b>	Titration Curve of 2-ThioUMP.....	45
<b>Figure 24</b>	Inhibition by 4-ThioUMP.....	46
<b>Figure 25</b>	Competitive Inhibition Model.....	36
<b>Figure 26</b>	$K_i$ Determination of 4-ThioUMP.....	46
<b>Figure 27</b>	Inhibition by 2-ThioUMP.....	47
<b>Figure 28</b>	Mixed Inhibition Model.....	36
<b>Figure 29</b>	$K_i$ Determination of 2-ThioUMP.....	47
<b>Figure 30</b>	Proposed Model for ODCase Decarboxylation.....	38
<b>Figure 31</b>	$^1\text{H}$ NMR Spectrum of Free ODCase.....	51
<b>Figure 32</b>	$^1\text{H}$ NMR Spectrum of ODCase/BMP Complex.....	51
<b>Figure 33</b>	$^1\text{H}$ NMR Spectrum of ODCase/UMP Complex.....	52



**List of Tables**

<b>Table 1</b>	Standard Bradford Assay .....	26
<b>Table 2</b>	Lysis Buffer .....	27
<b>Table 2a</b>	Lysis Buffer with Protease Inhibitors .....	27
<b>Table 3</b>	Ammonium Sulfate precipitation.....	27
<b>Table 4</b>	Dialysis Buffer .....	27
<b>Table 5</b>	12% SDS-PAGE.....	28
<b>Table 5a</b>	Staining Solution.....	28
<b>Table 5b</b>	Destaining Solution.....	28
<b>Table 6</b>	Purification of Wild Type ODCase .....	29
<b>Table 7</b>	Purification of Mutant ODCase .....	29
<b>Table 8</b>	Synthesis of 2-ThioUMP .....	40
<b>Table 9</b>	Absorbances of 4-ThioUMP and 2-ThioUMP.....	40
<b>Table 10</b>	pK <sub>a</sub> Determination .....	41-42
<b>Table 11</b>	K <sub>i</sub> Determination.....	42
<b>Table 12</b>	Inhibition Constants.....	43

**List of Symbols and Abbreviations**

$\beta$	beta
g	gram
mg	milligram
$\mu\text{g}$	microgram
nmol	nanomole
mL	milliliter
v/v	volume by volume
$\mu\text{L}$	microliter
$^{\circ}\text{C}$	degrees Centigrade
NMR	nuclear magnetic resonance
ppm	parts per million
nm	nanometer
$\mu\text{M}$	micromolar
M	molarity
cm	centimeter
w/w	weight by weight
L	liter
min	minute
sec	second
hr	hour
x g	gravitational force
kDa	kilodalton

**List of Symbols and Abbreviations (Continued)**

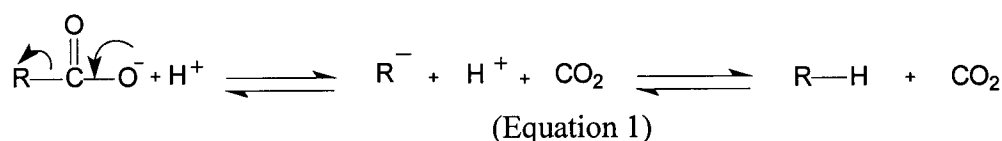
mM

millimolar

## Chapter 1 Introduction

### Decarboxylases:

Decarboxylation is the displacement of a carboxyl group by a proton with the formation of an anion intermediate whose stability determines the rate of the reaction (Equation 1).



The anion intermediate is usually a conjugated anion (often an enolate) in which the negative charge is located in a p-orbital that lies above and below a planar atomic framework (Figure 1).

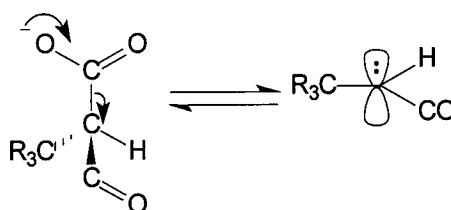


**Figure 1:** In decarboxylation, the enolate intermediate form has its negative charge lying in a p-orbital above the planar framework.

This implies that the carboxylate group in the substrate can either leave from the top or bottom of the system depending on the decarboxylase controlling this step. The stereochemistry of the decarboxylated product tells more about the decarboxylase. If the decarboxylation reaction occurs with retention of configuration then the same enzyme is responsible for removal of the carboxyl group and binding of the proton. On the other hand, inversion means that two separate enzymes catalyze each step. Racemization precludes the involvement of the decarboxylase in the proton transfer step.<sup>1</sup>

Decarboxylases have been classified into different categories depending on the course of their action.<sup>2</sup> The first class uses a divalent metal ion that acts as an electron sink as seen in the case of oxaloacetate decarboxylase (Figure 2). The uncatalyzed decarboxylation also uses  $Mg^{+2}$  to stabilize the intermediate and; therefore, is slower than the enzyme catalyzed reaction by a factor of  $10^8$ . This low proficiency leads to the suggestion that the enzyme's presence is necessary due to conformational and environmental factors.

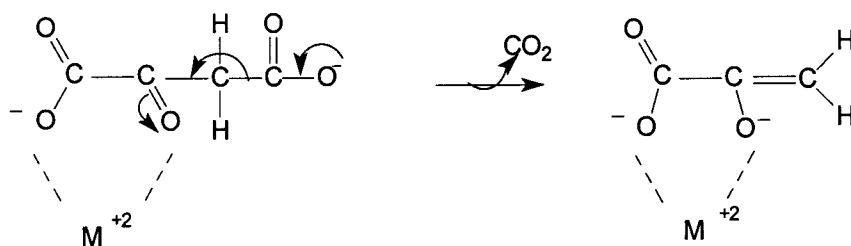


**Figure 2:** Oxaloacetate decarboxylase uses a divalent metal ion in its catalytic mechanism.

The second class involves an anion removal such as in the oxidative decarboxylation of 6-phosphogluconic acid to ribulose-5-phosphate catalyzed by phosphogluconate dehydrogenase. This enzyme uses  $NAD^+$  as an electron sink for the electron pair on the hydride ion being removed (Figure 3). Another enzyme that acts in the same way is malic enzyme that uses  $NADP^+$  in its oxidative decarboxylation of malic acid into pyruvic acid.

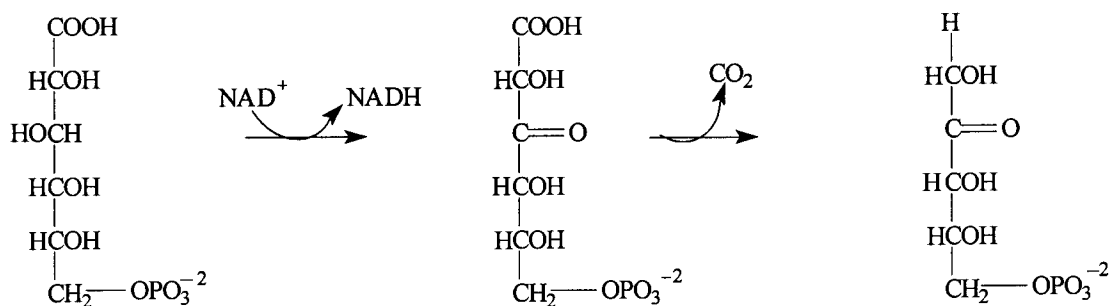


**Figure 3:**  $\text{NAD}^+$  as an electron sink for the hydride ion removed in the decarboxylation of 6-phosphogluconic acid.

The third class of decarboxylases uses a cofactor in its catalysis with one example being pyridoxal phosphate. Pyridoxal phosphate is involved in the decarboxylation of amino acids by forming a Schiff base with the amino acid. The electron pair formed in the decarboxylation is neutralized by the positive nitrogen of the pyridoxal (Figure 4). It is important to mention that the stereochemistry of the Schiff base intermediate determines whether the transamination or the decarboxylation of the amino acid is going to take place. In order for decarboxylation to be favoured, the carboxyl group of the amino acid should be out of the plane of the aromatic system while the  $\alpha$ -hydrogen and the alkyl group are on the other side of the plane (Figure 5). Transamination occurs with a different rotation of the groups around the  $\alpha$ -carbon of the amino acid and the nitrogen of the Schiff base.

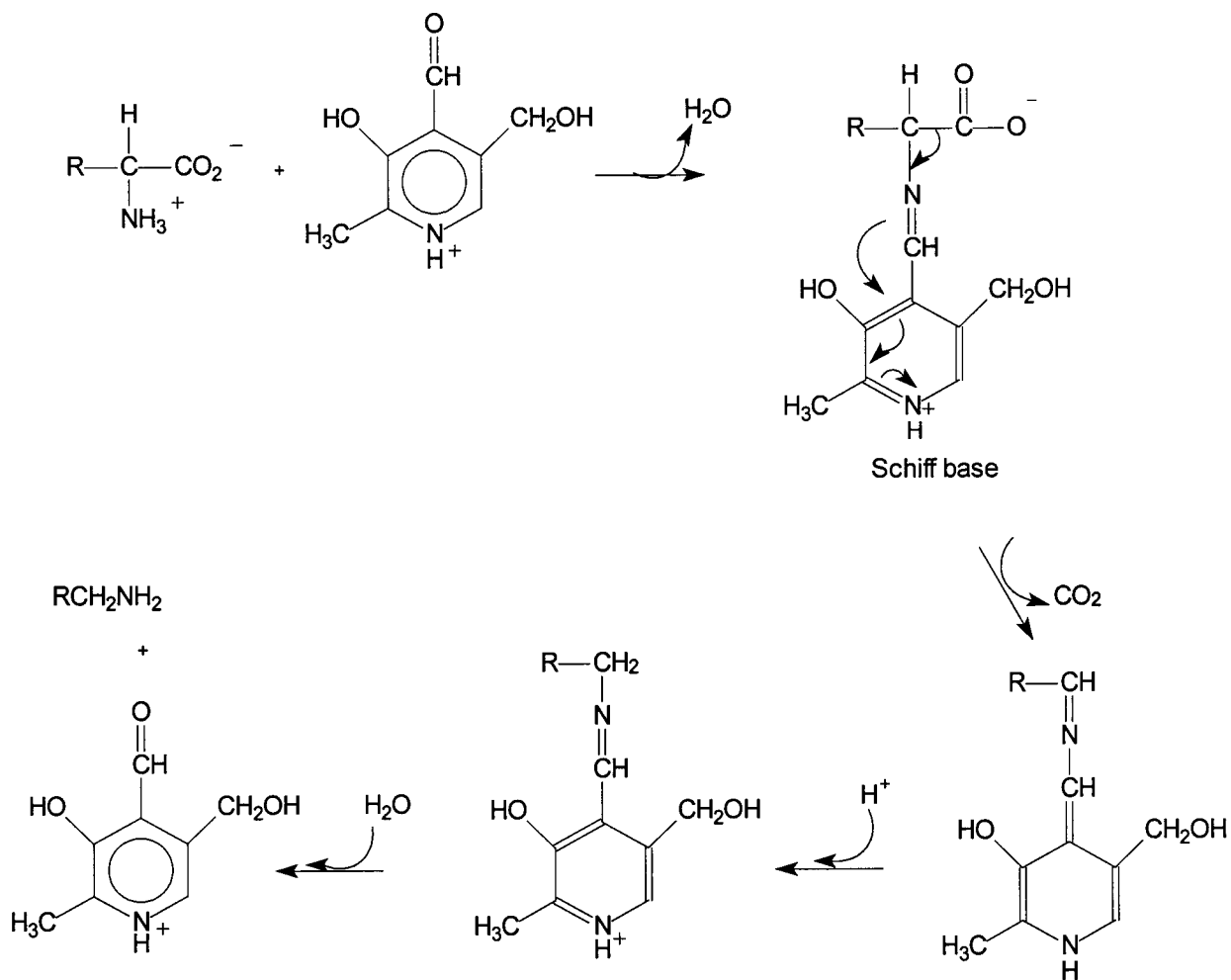


**Figure 4:** Amino acid decarboxylases use the cofactor pyridoxal phosphate in their catalysis.

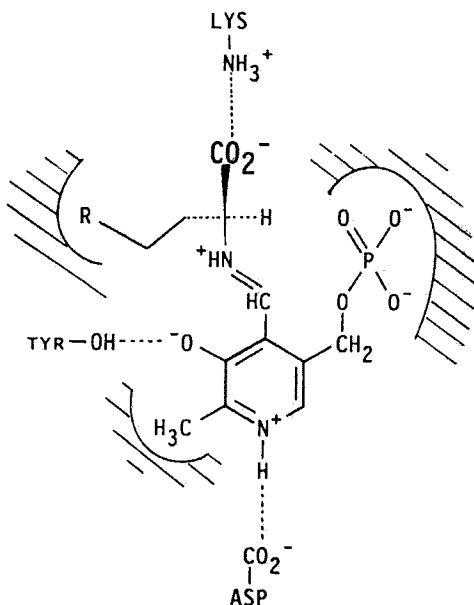


**Figure 5:** Conformation and stereochemistry of decarboxylation and projected active site of amino acid decarboxylase (from Sigman, D.S. (1992), "The Enzymes"<sup>1</sup>).

Another important cofactor found in decarboxylases is thiamine pyrophosphate (TPP). TPP is used by pyruvate decarboxylase to decarboxylate  $\alpha$ -keto acids. The highly active anionic form of TPP adds to the C-2 of pyruvate to form the intermediate shown in Figure 6. This step, rather than the decarboxylation, is the rate-determining step in the overall reaction. Upon decarboxylation of  $\alpha$ -keto acids a negative charge builds up on the carbonyl carbon that is stabilized by the delocalization of electrons on the ylide form of the thiazolium ring (Figure 6). The final product in the enzymic controlled reaction is acetaldehyde. Interestingly, the uncatalyzed reaction does not release an aldehyde but  $\alpha$ -hydroxyketone. It is thought that conformational control on the enzyme may be responsible for the formation of the aldehyde.



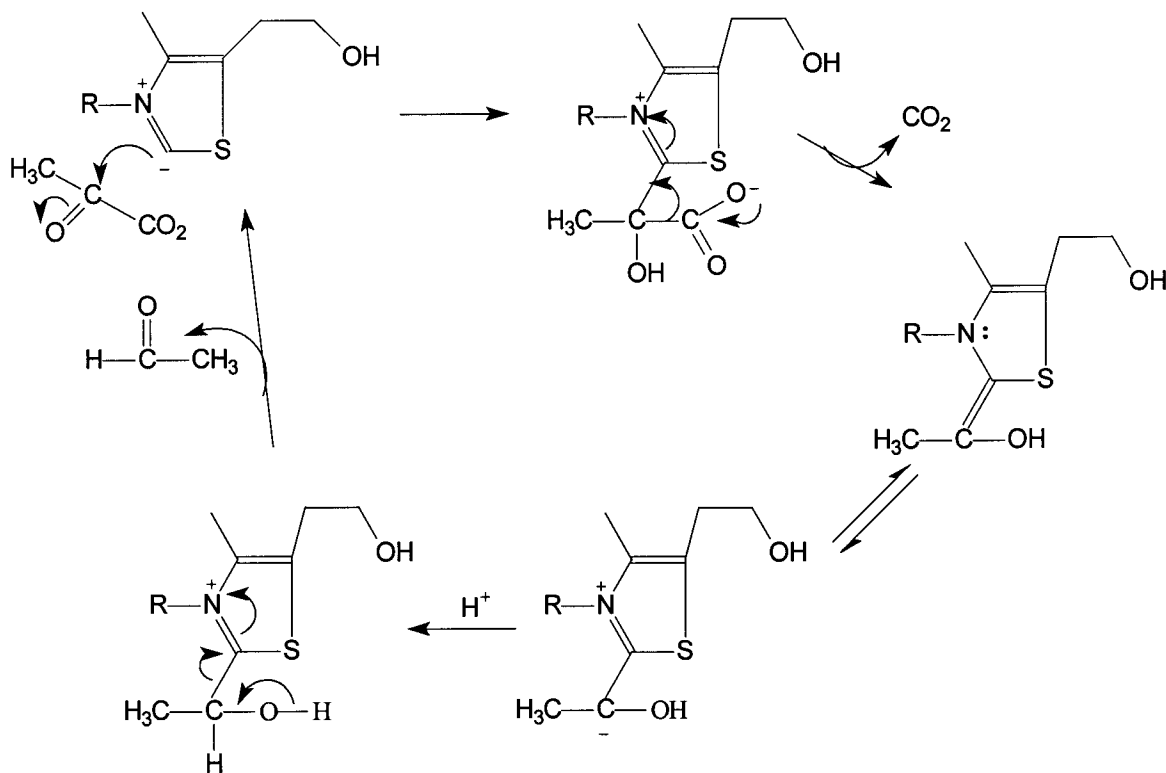


**Figure 6:** The mechanism of decarboxylation of pyruvate.

Extensive studies of different decarboxylases provide insight in understanding the mechanisms of decarboxylation. The most powerful techniques in such studies are X-ray crystallography and site-directed mutagenesis. This thesis focuses on the yeast enzyme orotidine 5'-monophosphate decarboxylase (ODCase) and different spectrophotometric studies carried out in the attempt of uncovering its catalytic mechanism.

### ODCase: Historical Background

Orotidine 5'-monophosphate decarboxylase catalyzes the conversion of orotidine 5'-monophosphate (OMP) into uridine 5'-monophosphate (UMP) in the final step of the *de novo* biosynthesis of pyrimidine nucleotides (Figure 7). UMP is a necessary precursor for all pyrimidine nucleotides in most organisms.<sup>3</sup>

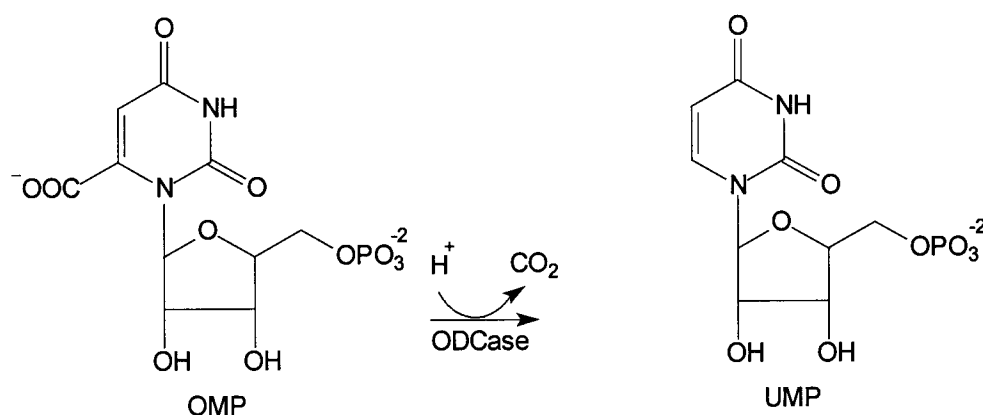


**Figure 7:** The last step in the *de novo* biosynthesis of pyrimidine nucleotides.

In bacteria and fungi, ODCase exists alone as a separate protein, whereas, in mammals it is a domain of a bifunctional protein, UMP synthase, which also catalyzes the preceding step in the *de novo* biosynthesis of UMP.<sup>4</sup> A study done by Kimsey and Kaiser on the amino acid sequence of ODCase from 20 different organisms revealed four conserved regions in all 20 sequences.<sup>5</sup> The deduced amino acid sequence of yeast ODCase shares 53-54% homology with the sequence of the ODCase domain of mouse and human UMP synthases.<sup>6</sup> Therefore, most research done on ODCase uses yeast as the source of this enzyme and mechanistic features are assumed to be similar for ODCases from all species.

The gene that codes for yeast ODCase, *ura3*, has been overexpressed by the vector pGU2 constructed by Lue *et al.*<sup>7</sup> On this plasmid the *ura3* gene is under the

control of *gal1* promoter, along with a region of the 2  $\mu$ m plasmid needed for maintenance at a high copy number in yeast, and *gal4* gene that encodes Gal4 protein (Figure 8).

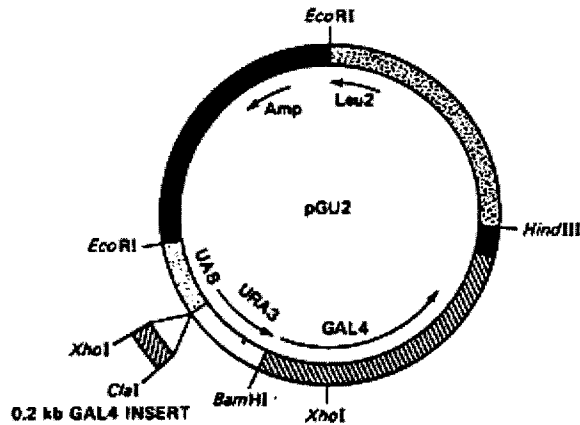


**Figure 8:** pGU2, a vector for the expression of Ura3 fusion proteins (from Lue *et al.*<sup>7</sup>).

The addition of galactose to the growth medium induces *gal 1* to promote the transcription of *ura3* and *gal4*, which, in turn, regulate the expression of a set of genes in *Saccharomyces cerevisiae*.

Although ODCase has been the subject of study of many enzymologists, its catalytic mechanism remains mysterious. Unlike other decarboxylases, ODCases have not yet been proven to involve either a cofactor or a metal ion in its action. Various mechanistic hypotheses had been proposed to explain the enormous rate enhancement by this enzyme. Lee and Houk suggested a mechanism involving protonation at the 4-oxygen position and formation of a stabilized carbene intermediate (Figure 9).<sup>8</sup>

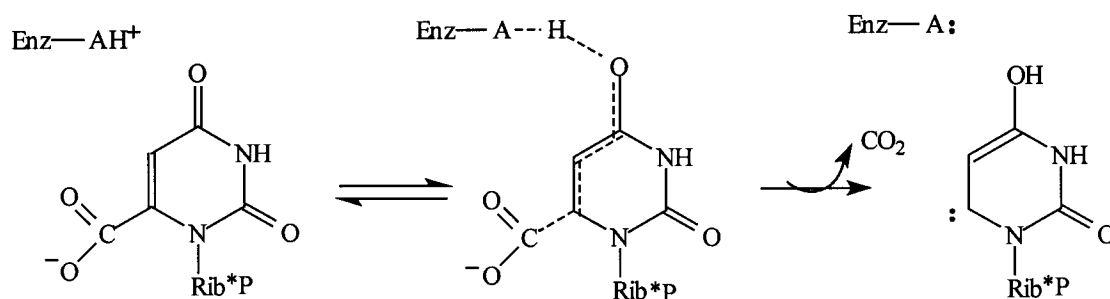


**Figure 9:** Lee and Houk's mechanism for decarboxylation by ODCase.

Their quantum mechanical calculations predicted that the decarboxylation of 4-protonated orotate was more favorable than the decarboxylation of 2-protonated orotate. The energetics of decarboxylation resulted from restricted Hartree-Fock (RHF) at the MP2 /6-31 + G\* + level. The  $\Delta H^\ddagger$  for the decarboxylation of orotate at 298 K was calculated to be 44.5 kcal mol<sup>-1</sup>, and the free energy of activation  $\Delta G^\ddagger$  was 38.4 kcal mol<sup>-1</sup> (experimental values were 44.4 and 38.5 kcal mol<sup>-1</sup>, respectively). The 2-oxygen protonation of orotate was shown to accelerate the reaction ( $\Delta G^\ddagger = 14.0$  kcal mol<sup>-1</sup>,  $\Delta H^\ddagger = 21.6$  kcal mol<sup>-1</sup>), however, the protonation at the 4-position drops the barrier for decarboxylation by an additional 6 kcal mol<sup>-1</sup> ( $\Delta G^\ddagger = 5.0$  kcal mol<sup>-1</sup>,  $\Delta H^\ddagger = 15.5$  kcal mol<sup>-1</sup>). Another reason that was presented to support their hypothesis was the fact that the 4-oxygen position in uracil is more basic than the 2-oxygen position.<sup>9</sup> Moreover, decarboxylation would increase the basicity of the oxygen and thus make it more susceptible to protonation.

Due to the lack of experimental evidence that would support Lee and Houk's carbene mechanism, our research group tends to reject this mechanism. We predict that the mechanism to be described below is more likely to occur. Two unique catalytic

mechanisms have been advanced for the enzymatic decarboxylation of OMP based on model compound studies. The first mechanism involves the formation of a nitrogen ylide intermediate (Figure 10) which acts as an electron sink to aid the breaking of the carbon-carbon bond.<sup>10</sup>

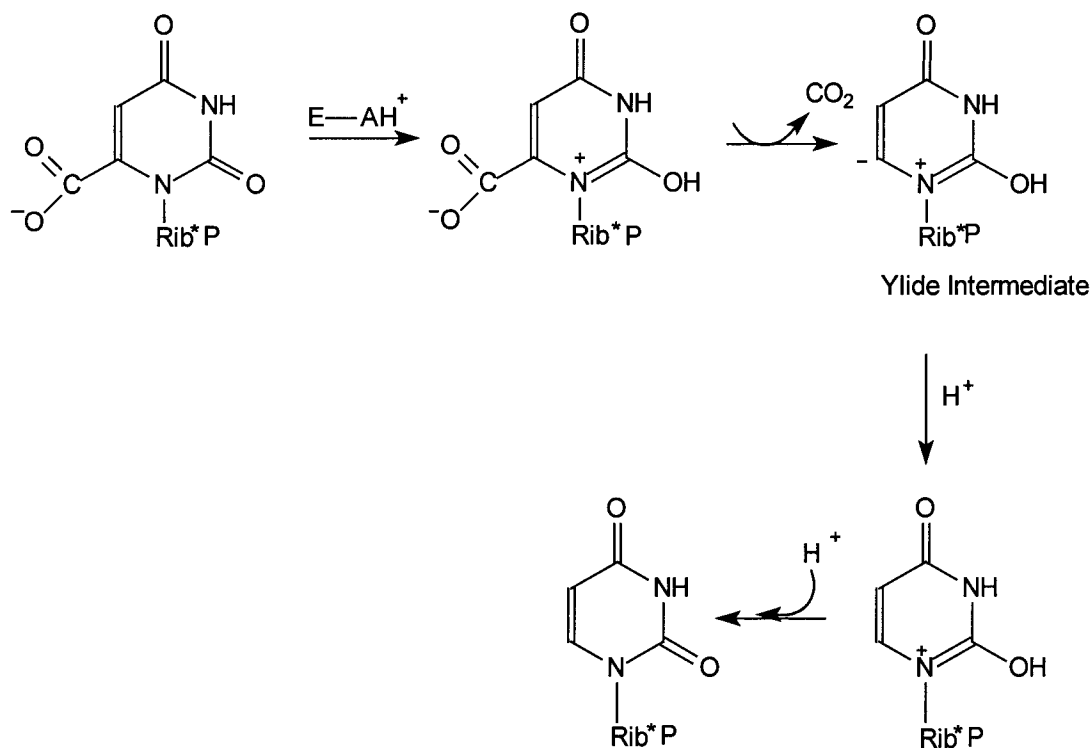


**Figure 10:** Decarboxylation of OMP by ODCase via a noncovalent Zwitterion/Ylide mechanism.

Ylide formation is proposed to occur by the protonation of the ketonic oxygen at C2 in the substrate, and no covalent bonds are formed between the enzyme and the substrate.

The second mechanism, which has been ruled out as a possibility<sup>11, 12</sup>, utilizes a nucleophilic residue to form a covalent enzyme-substrate adduct (Figure 11). In this mechanism, a Michael addition occurs at the 5-position of the substrate before the

elimination of the carboxyl group.<sup>13</sup> After decarboxylation, the enzyme-substrate bond is broken to release UMP.

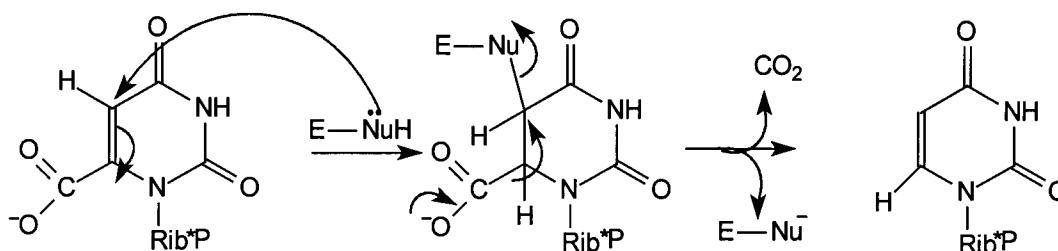


**Figure 11:** Beak and Siegel's addition- elimination mechanism

Several experiments were done in an attempt to distinguish between these two mechanisms; Levine *et al.* presented 1-(5'-phospho-β-D-ribofuranosyl) barbituric acid (BMP) as a very tightly bound, reversible inhibitor of the yeast enzyme owing to its resemblance to the intermediate shown in Figure 10.<sup>14</sup> Shostak and Jones, on the other hand, did studies on 5-azaOMP and they showed that in the presence of this suspected inhibitor an enzyme-dependent reaction occurs, presumably decarboxylation (the final products of the reaction had not been identified). This enzyme reaction follows Michaelis-Menten kinetics. Because the 5-aza group is not electrophilic, an enzyme mechanism utilizing a nucleophilic addition of the enzyme at the 5-position is ruled out.<sup>12</sup> Moreover, spectral studies done by the same group to explore the interaction between the enzyme and 6-azauridylate (6-azaUMP), a potent inhibitor, again provided evidence against the mechanism involving loss of the double bond between the 5 and 6 position since the UV absorption was maintained in the bound inhibitor. Acheson *et al.* investigated the kinetic isotope effect on the catalytic mechanism of ODCase. ODCase

was titrated with the  $^{13}\text{C}$ -enriched BMP, and only a small downfield displacement (0.6 ppm) of the C-5 resonance was observed, indicating that no addition by an enzymic nucleophile occurred at C-5 of the inhibitor. Kinetic effects of hydrogen substitution with deuterium at C-5 have been used to detect the changes in hybridization of reacting centers in OMP. No significant changes in  $k_{\text{cat}}$  or  $k_{\text{cat}}/K_{\text{m}}$  were found to result, suggesting that C-5 does not undergo significant changes in geometry before or during the step that determines the rate of the catalytic process.<sup>15</sup>

The above experiments led our group to investigate the Ylide/Zwitterion mechanism. In this mechanism, the enzyme provides an environment in which the basicity of the substrate's 2-oxygen is increased so that the active site residue would protonate the keto group. This increase would be facilitated by a hydrophobic active site or the presence of a metal ion to stabilize the zwitterionic transition state. Miller *et al.* were able to prove that  $\text{Zn}^{+2}$  does exist in yeast ODCase, however, its exact position could not be determined.<sup>16</sup> Cleland and Kreevoy suggested that protonation is concerted with decarboxylation, and not a distinguishable pre-decarboxylation step. The concerted mechanism may overcome the thermodynamic barrier of proton transfer from the amino acid on the active site (a lysyl protonated amine of  $\text{pK}_{\text{a}} \cong 7$ )<sup>17</sup> and the carbonyl oxygen.<sup>18</sup> This proton transfer may be in the form of a "short, strong hydrogen bond" known as a Low Barrier Hydrogen Bond (LBHB).<sup>19</sup> This unusually strong hydrogen bond may contribute to the enzyme's stabilization of the transition state versus the ground state.

Smiley and Jones substituted Lys 93 of yeast ODCase with a cysteine, in a site directed mutagenesis experiment.<sup>17</sup> Lys 93 is one of the invariant amino acids in all ODCase sequences.<sup>7</sup> The resulting mutant protein (K93C) showed a decrease in activity

by a factor of  $2 \times 10^{-8}$  times the activity of the wild-type enzyme. In contrast to the wild type, K93C protein displayed no binding preference for 6-azaUMP over UMP. It is also worth noting that the mutation does not drastically affect the enzyme's structure or its affinity for substrate. To summarize, evidence has been presented for a catalytic role of Lys 93 of yeast ODCase as a proton donor in catalysis, and, is an integral portion of the active site.

As a conclusion, this great catalytic power of ODCase must be owed to certain stabilization factors. Our research group suspects that this rate enhancement is due to a LBHB formed between the enzyme and the transition state. Spectroscopic studies will be described in the following chapters in an attempt to confirm our hypothesis. However, several questions will remain unanswered and many future approaches shall be taken by interested biochemists to answer them.

#### The Low Barrier Hydrogen Bond:

The low barrier hydrogen bond- also known among physical chemists as the "proton shared hydrogen bond" is a short, strong hydrogen bond. This hydrogen bond is suspected to be formed in enzyme-catalyzed reactions for which the uncatalyzed free energy of formation in solution is more positive than the free energy of activation of the catalyzed reaction.<sup>20</sup> Due to the strength of this LBHB, stabilization of the enzyme-bound intermediate compared to the initial enzyme-substrate complex occurs. The strength of the LBHB is attributed to its length, linearity, microenvironment, and the  $pK_a$ 's of the conjugate acids of the heteroatoms sharing the proton.<sup>19</sup> The shorter a bond the stronger it is, and a LBHB is shorter than a normal hydrogen bond. The O...H...O distance for a weak hydrogen bond is 2.8 to 3.0 Å, whereas that for a strong hydrogen



bond is  $< 2.5 \text{ \AA}$ .<sup>18</sup> The strongest bonds are also formed between bases of similar or matching proton affinities. It is true that the proton affinities of the two basic sites may be quite different in the enzyme-substrate complex, however, they become more similar as the enzyme-intermediate complex is formed.<sup>20</sup> Moreover, the LBHB has distinct physiochemical properties in addition to its short heteroatom distance. Its infra red (I.R.) absorption spectrum contains a very broad and intense hydroxyl absorption band between  $2000 \text{ cm}^{-1}$  and  $500 \text{ cm}^{-1}$ ; instead of the usual  $3000\text{-}2000 \text{ cm}^{-1}$ .<sup>20</sup> Also, its  $^1\text{H}$  NMR chemical shift is far downfield (17-21 ppm) from tetramethylsilane (TMS).<sup>18</sup> The strength of the hydrogen bond is correlated with NMR chemical shifts determined by theoretical calculations.<sup>21</sup> A LBHB is also characterized by a low deuterium fractionation factor indicating deuterium is not easily exchanged with the protium ( $^1\text{H}$ ) in the already existing hydrogen bond.<sup>18</sup> In conclusion, low barrier hydrogen bonds may be very important in explaining enzymatic rate enhancement. They stabilize intermediates in enzymatic reactions and lower the energy of formation of transition states. These bonds can be identified by their short interatomic distances, low fractionation factors, and by physical methods such as infrared and NMR spectroscopy.

## Chapter 2 Yeast ODCase Purification and Stabilization

### Introduction:

Orotidine -5'-monophosphate decarboxylase (ODCase) was prepared from yeast strain BJ5424 transformed with plasmid pGU2 which carries the *ura 3* gene for ODCase.<sup>7</sup> The yeast cultures were induced with galactose and then followed with cell lysis. ODCase was purified by ammonium sulfate fractionation 60-90% and affinity chromatography on an Affi-Gel Blue column as previously described.<sup>6</sup> 6-azaUMP was used to elute ODCase from this column and the fractions containing this enzyme were pooled, concentrated, and chromatographed on a MonoQ anion exchange column using the Pharmacia FPLC system. ODCase emerged at the beginning of a 0-200 mM NaCl gradient, with 10 mM potassium phosphate, pH 7.5, 10% (v/v) glycerol, and 5 mM  $\beta$ -mercaptoethanol all present in both gradient buffers.<sup>22</sup> 6-azaUMP and phosphate used in the purification steps were removed by exhaustive dialysis with multiple changes of the buffer containing 50 mM Tris buffer at pH 7.4, 10% (v/v) glycerol, 5mM  $\beta$ -mercaptoethanol, and 10 mM UMP, and then 50 mM Tris buffer at pH 7.4, 10% (v/v) glycerol, and 5mM  $\beta$ -mercaptoethanol only. The specific activity of ODCase was between 15-20 nmol min<sup>-1</sup>  $\mu$ g<sup>-1</sup>.

Mutant ODCase was obtained after the induction of yeast BJ5424/ K93C cells with galactose.<sup>17</sup> The mutant protein (K93C) was prepared by site-directed mutagenesis where Lys93 (encoded by the yeast plasmid pGU2) was replaced with a cysteine and so the sequence was as follows: K93C, 5'GAAGACAGATGTTTTGCTGAC-3'.<sup>17</sup> The purification process was mainly the same as the wild type ODCase. Ammonium sulfate fractionation was followed by dialysis, then column chromatography with Affi-Gel Blue

and MonoQ columns. Since the mutant ODCase did not bind to the Affi-Gel Blue column it emerged in the very first fractions, and 6-azaUMP was not needed nor was the exhaustive dialysis step. Purity of the mutant protein was judged by commassie blue stained polyacrylamide gels. Protein concentration was determined by the dye binding method of Bradford, using bovine serum albumin (BSA) as standard.<sup>22</sup>

#### Affinity Chromatography:

Affinity chromatography gets its name from its function where the inert solid support is covalently linked to a biologically specific ligand. Upon application on the column, molecule(s) with an affinity for the ligand bind specifically and reversibly to it while the rest of the molecules pass through. The substance of interest can be eluted by changing the pH, ionic strength, or by addition of a competing ligand. Affinity chromatography is used in the purification and isolation of enzymes, antibodies, antigens, nucleic acids, polysaccharides, coenzyme or vitamin binding proteins, repressor proteins, transport proteins, drug or hormone receptor structures, and other biochemical materials.<sup>23</sup>

The purification of yeast ODCase required the use of an Affi-Gel blue column. Affi-Gel blue is a beaded, cross-linked agarose gel with covalently attached Cibacron Blue F3GA dye (Figure 12). The Affi-Gel blue gel purifies a large range of proteins from widely divergent origins. The blue dye functions as an ionic, hydrophobic, aromatic, or sterically active binding site in various applications. Proteins that interact with Affi-gel blue gel can be bound or released with a high degree of specificity by manipulating the composition of the eluant buffers.

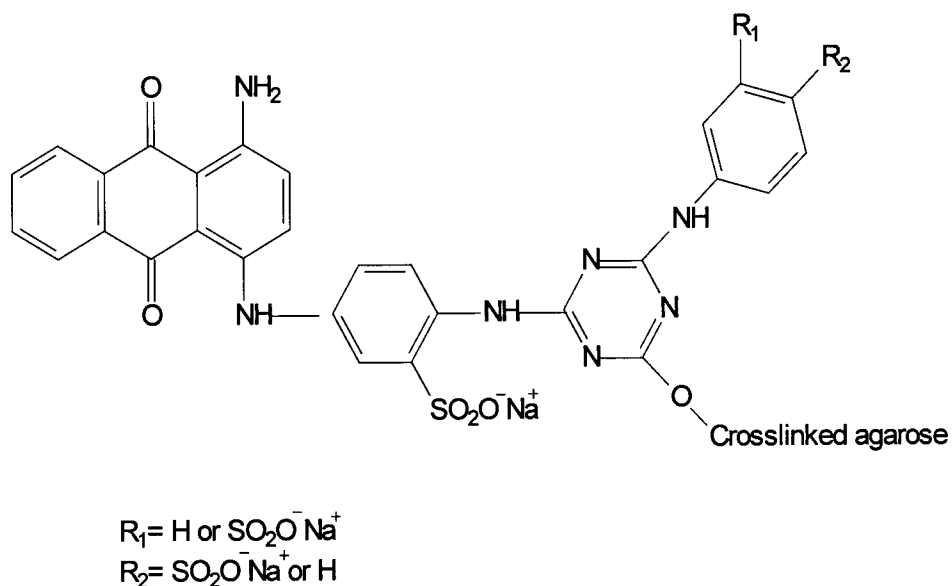


**Figure 12:** Cibacron blue coupled to agarose in the Affi-Gel Blue column.

#### Ion Exchange Chromatography:

Proteins are polyionic molecules that carry both positive and negative charges. This ionic characteristic allows their purification by ion exchange chromatography. In this process the solid inert matrix is chemically linked to charged groups bound to ion exchangers. The ion exchangers are either positively charged (cation exchangers) or negatively charged (anion exchangers). The type of exchanger to which a specific protein sample might bind depends on the net charge of this protein at the pH used in the chromatography buffer. Positively charged proteins will bind to cation exchangers whereas negatively charged proteins will bind to anion exchangers. The pH and salt concentration of the buffer solution that contains the protein sample also affect the binding affinity of the protein. Since the charged protein groups are acid-base groups, they are highly affected by pH variation and so is the net charge of the protein. Once the

protein sample is applied on the ion exchange column, proteins with low affinity will pass through the column while high affinity proteins stay on it, a process known as “elution”. Following elution is “Stepwise elution” in which the column is washed by buffers of different salt concentrations (and/or different pH's) in attempts to elute the protein of interest.<sup>22</sup>

Fast Protein Liquid Chromatography (FPLC) was one form of chromatographic techniques used in the purification of yeast ODCase. To operate this FPLC system a Mono Q HR 5/5 column had been used. It is an anion exchange liquid chromatography column that acts as a strong anion exchanger based on a beaded hydrophilic resin with a particle size of 10  $\mu\text{m}$  and a positively charged group on its gel  $[-\text{CH}_2-\text{N}^+(\text{CH}_3)_3]$ .

#### SDS-Polyacrylamide Gel Electrophoresis:

Electrophoresis separates biological molecules based on their charge and frictional coefficient. In polyacrylamide gel electrophoresis (PAGE), gels are made by the polymerization of polyacrylamide that is induced by ammonium persulfate (APS) which in turn is catalyzed by N,N,N',N'-tetramethylethylenediamine (TEMED). Sodium dodecyl sulfate (SDS)  $[\text{CH}_3-(\text{CH}_2)_{10}-\text{CH}_2-\text{O}-\text{SO}_3^-]\text{Na}^+$  is a detergent that denatures proteins and causes them to assume a rod-like shape. All SDS- treated proteins would have identical charge- to- mass ratios and similar shapes. Therefore, in SDS-PAGE proteins would be separated based on their molecular weights, where those with lower molecular weights migrate farther.<sup>23</sup>

#### The Bradford Assay:

The dye used in this method Coomassie brilliant blue G-250, exists in, a red form ( $A_{\text{max}}= 465 \text{ nm}$ ) when in solution. Once it binds to protein it shifts to the blue form

( $A_{\max} = 595 \text{ nm}$ ). Table 1 describes the preparation of solutions used in Bradford assay. A Hewlett Packard 8452 A diode array spectrophotometer was used to take absorbance readings.

#### Materials:

Phenylmethylsulfonyl fluoride (PMSF), pepstatin A, leupeptin, and BSA were purchased from Sigma. Yeast extract, bacto-peptone, bacto agar, glucose, and galactose were from Fisher Biotech. Yeast nitrogen base without amino acids was from Difco. Affi-Gel Blue was from Bio-rad. Glycerol and ammonium sulfate were from Amresco. Yeast strain BJ5424 was from Yeast Genetic Stock Center, University of California, Berkeley.

#### Yeast Growth Protocol:

The transformed yeast cells with the pGU2 plasmid were selected according to their ability to grow on a synthetic complete medium agar plate containing 2% (w/w) glucose in the absence of leucine (Leu) and uracil. Synthetic complete medium (SCM) consists of 1.44 g/L dropout powder containing: 4% adenine, tryptophan, histidine, arginine, and methionine; 6% tyrosine, lysine, and isoleucine; 10% phenylalanine and valine; and 40% threonine<sup>7</sup>, 1.89 g/L yeast nitrogen base without amino acids, 5.56 g/L ammonium sulfate, all dissolved in H<sub>2</sub>O and adjusted to pH 6.0. SCM/agar is prepared by the addition of 16.7 g/L agar to the above SCM medium. Colonies appeared in 3-4 days and were picked and grown at 30°C in a Fisher Isotemp incubator model 2550 in a 10 mL of SCM/glucose (10% (v/v) glucose) medium for 24 hr. 1 mL of this culture was then transferred into three 30-mL aliquot of SCM containing 3 mL of 2% (w/w) sucrose at 30°C with shaking for 16 hr. Following that 20 mL of SCM/sucrose culture was

transferred into each of four 900-mL flasks of Yeast/Peptone (YP) medium consisting of 11.0g/mL yeast extract, 22.2 g/mL peptone, 11% (v/v) of 2% (w/w) sucrose. This culture was in turn incubated at 30° C with shaking for 12 hr. 100 mL of 2% (w/w) galactose was added and incubation was continued for 9-10 hr. Yeast cells were collected by centrifugation and either lysed or frozen at -20° C.

BJ5424 cells producing the mutant enzyme ODCase K93C were selected by their ability to grow on a SCM/ glucose agar plate in the absence of Leu. They were then incubated in a 9 mL YP/glucose (10% (v/v) glucose) medium at 30°C until it was viscous. 1 mL of the YP/glucose medium was transferred into 10 mL of SCM/ glucose (10 % (v/v) glucose) medium. The remaining steps were the same as the steps for the growth protocol for the wild type enzyme. The only difference was that the SCM medium used in the mutant growth protocol contained 0.72g/L uracil. The mutated *ura3* gene does not allow growth in the absence of uracil, and thus it is essential to add it to the growth medium.

#### Purification of Yeast ODCase:

Yeast ODCase was obtained from the organism *Saccharomyces cerevisiae* strain BJ5424 transformed with plasmid pGU2, which carries the *ura3* gene for ODCase. The yeast cells were grown according to the yeast growth protocol. These cells were harvested in preweighed centrifuge bottles at 6000 x g for 10 min at a temperature of 4°C in a Sorvall RC 5B Plus. The weighed pellets were resuspended in lysis buffer (Table 2) and ruptured using a bead beater (Biospec products): 7x 60 sec interspersed with 60 sec interval for cooling. Cell debris was removed by centrifugation at 10000 x g for 20 min and the supernatant was fractionated using solid ammonium sulfate. The 60-90%

precipitate (Table 3) was then collected in 2-3 ml lysis buffer /protease inhibitors (Table 2a) and was dialyzed against 1L dialysis buffer (Table 4) for about 18 hr to remove any ammonium sulfate traces. The dialyzed protein fraction was then applied to an Affi-Gel Blue column (1.5 x 20 cm). Non-specific binding proteins were removed from the column by 180-200 ml dialysis buffer while ODCase was eluted by 200 mL of the same buffer containing 50  $\mu$ M aza-UMP. The Affi-Gel Blue column was then washed with 150 mL high salt dialysis buffer (200 mM + dialysis buffer) to remove traces of proteins still stuck on the column, then with 150 mL dialysis buffer to retain its initial pH. Fractions containing ODCase were identified by 12% SDS- polyacrylamide gel (Tables 5, 5a, and 5b). The pure ODCase monomer had a molecular weight of 29,500 daltons<sup>6</sup> in agreement with its migration on the gel (Figure 13). The ODCase fractions were then concentrated to a volume of 4 mL by using an Amicon Stirred Cell Ultrafiltration apparatus and Diaflo Ultrafiltration membrane. The aza-UMP was removed by sequential dialysis against 400 mL dialysis buffer with 10mM UMP (buffer's volume is 100 fold excess over the enzyme's volume) for 48 hr with change of buffer every eight hours. This fraction was dialyzed against the same volume of dialysis buffer (without UMP) for about 12 hr. The dialyzed fraction was then applied on an FPLC column. ODCase emerged at the beginning of a 0-200 mM NaCl gradient, with 10 mM potassium phosphate, pH 7.5, 10% (v/v) glycerol, and 5 mM  $\beta$ - mercaptoethanol present in both gradient buffers (Table 2). Fractions from the FPLC column were electrophoresed 12% SDS-polyacrylamide gel and bands were visualized with Coomassie staining (Figure 14). The FPLC fractions containing ODCase were further concentrated to a final volume of 1-2 mL (Figure 15). If the gel from the affinity column did not show



any contaminating proteins (Figure 16) then the FPLC purification step might not be needed. Instead, the ODCase fractions from the Affi-Gel Blue column were dialyzed and concentrated to 1-2 mL. In a typical purification, 90 g of yeast cells (WT) resulted in 1.5 ml of 17 mg/mL purified ODCase (Table 6). Purified ODCase can be kept frozen at -20°C with 20% (v/v) glycerol and will retain most of its activity for 3-4 months.

After growing the mutant protein cells according to the protocol described previously, the cells which weighed 52.755 g were lysed in a bead beater: 7x60 sec interspersed with cooling 60 sec cooling interval. The lysis solution was then centrifuged at 10000 x g for 20 min at 4°C in the Sorvall centrifuge to get rid of the debris. The pellet was discarded while the supernatant was kept for 60-90% fractionation with solid ammonium sulfate. The pellet was then collected in a small volume of lysis buffer with protease inhibitors. This solution was dialyzed overnight against 1L dialysis buffer. The Affi-Gel Blue gel column was then used, however, the mutant ODCase did not bind to the column but emerged in the very first fractions after washing the column with dialysis buffer. These fractions were run on 12% SDS-PAGE gels and showed big ODCase bands with impurities (Figure 17). These fractions were concentrated using an Amicon Stirred Cell Ultrafiltration apparatus and Diaflo Ultrafiltration membrane up to 4 mL (Figure 18). The concentrated fraction was run on the FPLC system and similar to the wild type it emerged at the beginning of the gradient buffers (Table 2). The Bradford assay was used to determine the concentration of mutant protein at each step (Table 7).

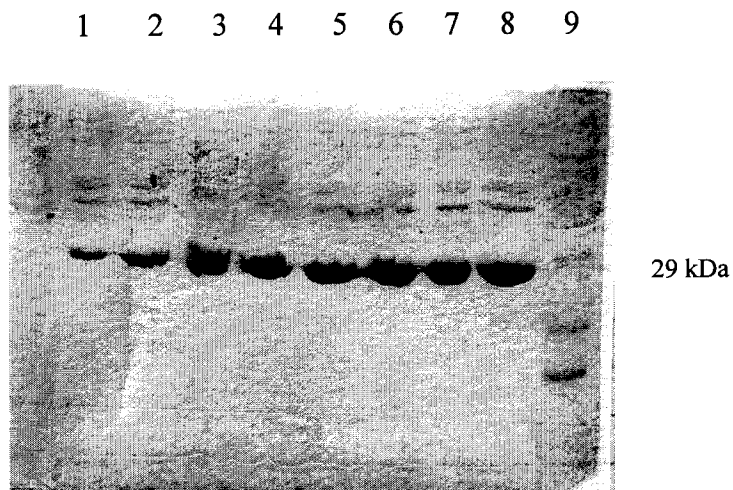


**Figure 13:** Wild type ODCase purified by Affi- Gel Blue chromatography (Lanes 1 to 8) was run on 12% SDS-polyacrylamide gel and coomassie blue stained. Molecular weight markers are positioned in *lane 9*. The wide bands in *lanes 2 to 8* represent the ODCase monomer of 29,000 daltons.

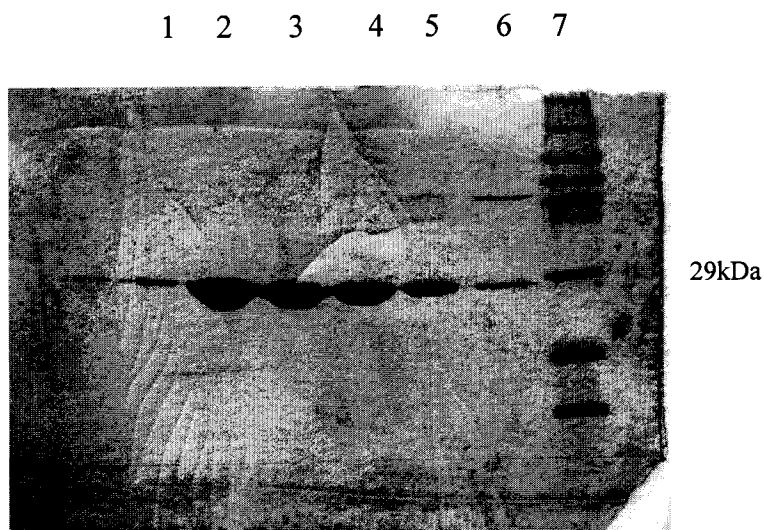


**Figure 14:** Wild type ODCase purified by FPLC system (Lanes 1 to 6) was run on 12% SDS-polyacrylamide gel and coomassie blue stained. Molecular weight markers are positioned in *lane 7*. The wide bands in *lanes 2 to 5* represent the ODCase monomer of 29,000 daltons.

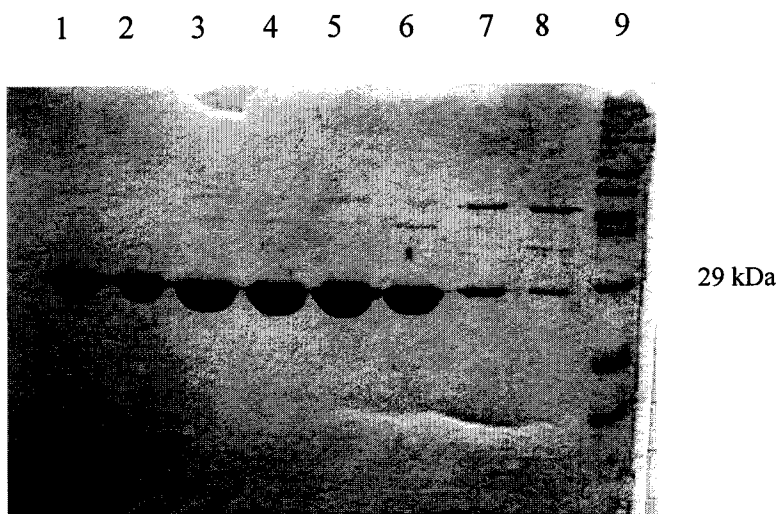


**Figure 15:** Pooled wild type ODCase (Lanes 1 to 8) was run on 12% SDS-polyacrylamide gel and coomassie blue stained. Molecular weight markers are positioned in *lane 9*. The wide bands in *lanes 1 to 6* represent the ODCase monomer of 29,000 daltons.

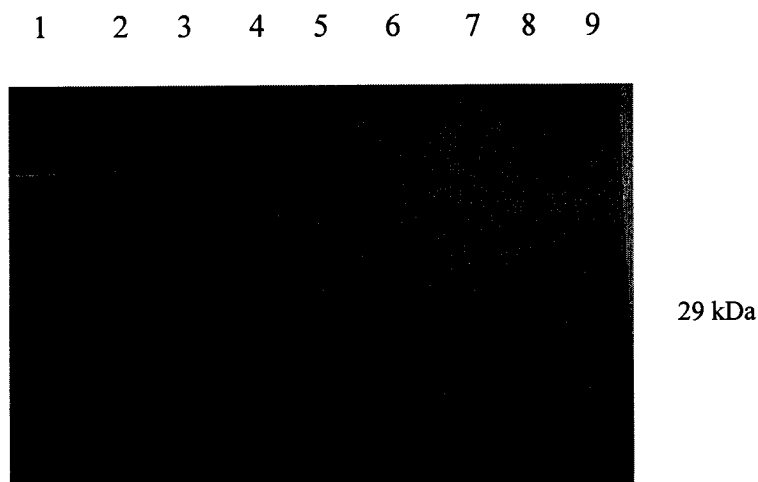


**Figure 16:** Wild type ODCase purified by Affi- Gel Blue chromatography (Lanes 1 to 8) was run on 12% SDS-polyacrylamide gel and coomassie blue stained. Molecular weight markers are positioned in *lane 9*. The wide bands in *lanes 1 to 8* represent the ODCase monomer of 29,000 daltons. There is no trace of contaminating proteins in these lanes.

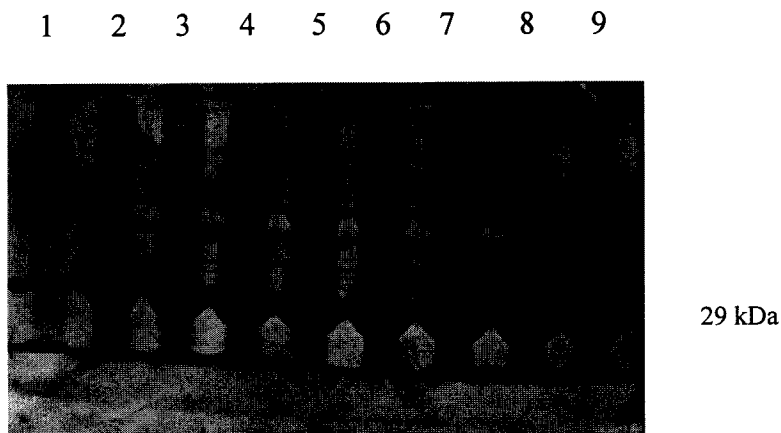


**Figure 17:** Mutant ODCase (K93C) purified by Affi- Gel Blue chromatography (Lanes 2 to 8) was run on 12% SDS-polyacrylamide gel and coomassie blue stained. Molecular weight markers are positioned in *lane 1*. *Lanes 2 to 8* show wide bands of mutant ODCase monomers at 29,000 daltons as well as a lot of contaminating proteins.

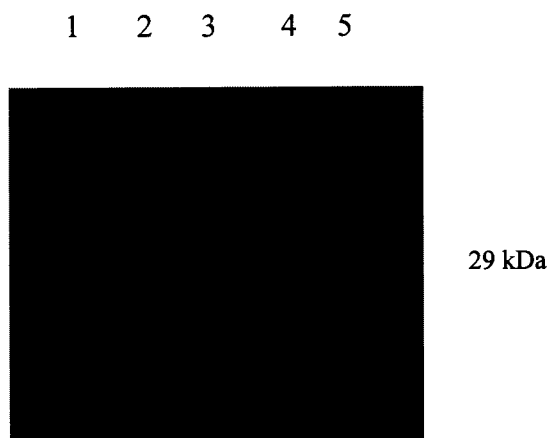


**Figure 18:** *Lanes 1 to 4* represent pooled, mutant ODCase (K93C) on a 12% SDS-polyacrylamide gel. *Lane 1 and 2* show wider mutant ODCase monomer bands (higher protein enzyme concentration) at 29,000 daltons than *lanes 3 and 4*. Molecular weight markers are positioned in *lane 5*.

**Table 1: Preparation of Bradford assay (standard)**

Sample	Volume of 0.5 mg/mL Bovine serum albumin (BSA) in $\mu\text{L}$	Volume of 0.15 M NaCl in $\mu\text{L}$	Volume of coomassie blue G-250 in $\mu\text{L}$
1	0	100	900
2	5	95	900
3	10	90	900
4	15	85	900
5	20	80	900
	<b>Volume of protein sample</b>		
	V	100-V	900

**Sample Bradford assay calculation**

Volume of BSA in $\mu\text{L}$	Mass of BSA in $\mu\text{g}$	Absorbance at 596 nm
0	0.0	0.00673
5	2.5	0.18387
5	2.5	0.20810
10	5.0	0.35562
10	5.0	0.35165
15	7.5	0.51155
15	7.5	0.51166
20	10.0	0.63173
20	10.0	0.62775
Volume of protein sample in $\mu\text{L}$	Mass of protein sample in $\mu\text{g}^a$	Absorbance at 596 nm
5	M	0.49457
<b>Mathematical operation, calculation of the protein mass</b>	$M = (0.49457 - 0.036) / 0.0613 = 7.60$	

<sup>a</sup> Mass of the protein was calculated by using the linear equation obtained upon plotting the above data (Figure 19)

**Table 2: Lysis Buffer (The same concentrations were used for the FPLC system buffer)**

Compound	Concentration
Potassium monophosphate buffer pH= 7.4	50 mM
Glycerol	10% (v/v)
$\beta$ -mercaptoethanol	5 mM

**Table 2a: Lysis Buffer with protease inhibitors**

When protease inhibitors are added to lysis buffer, the following concentrations are used:

Compound	Concentration
Pepstatin	2 $\mu$ M
Leupeptin	0.6 $\mu$ M
Phenyl methyl sulfonyl fluoride (PMSF)	1 mM

**Table 3: 60-90% Solid ammonium sulfate precipitation<sup>a</sup>**

% Saturation	Volume of Supernatant in mL	Concentration of $(\text{NH}_4)_2\text{SO}_4$ to be added in g/mL	Mass of $(\text{NH}_4)_2\text{SO}_4$ added in g
60	200	0.361	72.20
90	226	0.221	49.95

<sup>a</sup>Sample calculation from an experiment done using the supernatant solution obtained upon the lysis of 90 g yeast cells

**Table 4: Dialysis buffer**

Compound	Concentration
TRIS ((hydroxymethyl)aminomethane buffer pH= 7.4	50 mM
Glycerol	10% (v/v)
$\beta$ -mercaptoethanol	5 mM

**Table 5: Preparation of 12% SDS- PAGE**

Compound	Amount needed for 1 gel
<b>Resolving Gel (lower gel)</b>	
Lower Tris buffer (1.5 M at pH 8.8)	1.9 mL
40% acrylamide solution	2.3 mL
H <sub>2</sub> O	3.4 mL
Ammonium persulfate	100 $\mu$ L
TEMED	10 $\mu$ L
<b>Stacking Gel (upper gel)</b>	
Upper Tris buffer (0.5 M at pH 6.8)	1.25 mL
40% acrylamide solution	0.75 mL
H <sub>2</sub> O	2.9 mL
Ammonium persulfate	50 $\mu$ L
TEMED	10 $\mu$ L

**Table 5a: Coomassie blue staining solution**

Compound	Concentration (v/v)
Methanol	50%
Coomassie brilliant blue G-250	0.05%
Acetic acid	10%
H <sub>2</sub> O	40%

**Table 5b: Destaining solution**

Compound	Concentration (v/v)
Methanol	5%
Acetic acid	7%
H <sub>2</sub> O	88%

**Table 6: Sample Purification of wild type yeast ODCase<sup>a</sup>**

<b>Fraction</b>	<b>Concentration in <math>\mu\text{g}/\mu\text{L}^{\text{b}}</math></b>	<b>Volume in mL</b>
Dialyzed Ammonium Sulfate	6.01	38.3
Affi-Gel Blue	2.04	20
FPLC	2.54	22
Dialyzed, pooled ODCase	9.49	2.63
Dialyzed, pooled ODCase	17	1.50

<sup>a</sup>90 g of yeast cells from 4.8 L YP medium plus 20% sucrose were harvested after 9 h of galactose induction and processed as described in the text

<sup>b</sup>Concentration in  $\mu\text{g}/\mu\text{l}$  was obtained by Bradford assay calculations

**Table 7: Sample Purification of mutant yeast ODCase<sup>a</sup>**

<b>Fraction</b>	<b>Concentration in <math>\mu\text{g}/\mu\text{L}</math></b>	<b>Volume in mL</b>
Lysate	4.73	5
Pooled Affi-Gel Blue	19.2	4
FPLC	7.32	3

<sup>a</sup>53 g of yeast cells from 4.8 L YP medium plus 20% sucrose were harvested after 9 hr of galactose induction and processed as described in the text



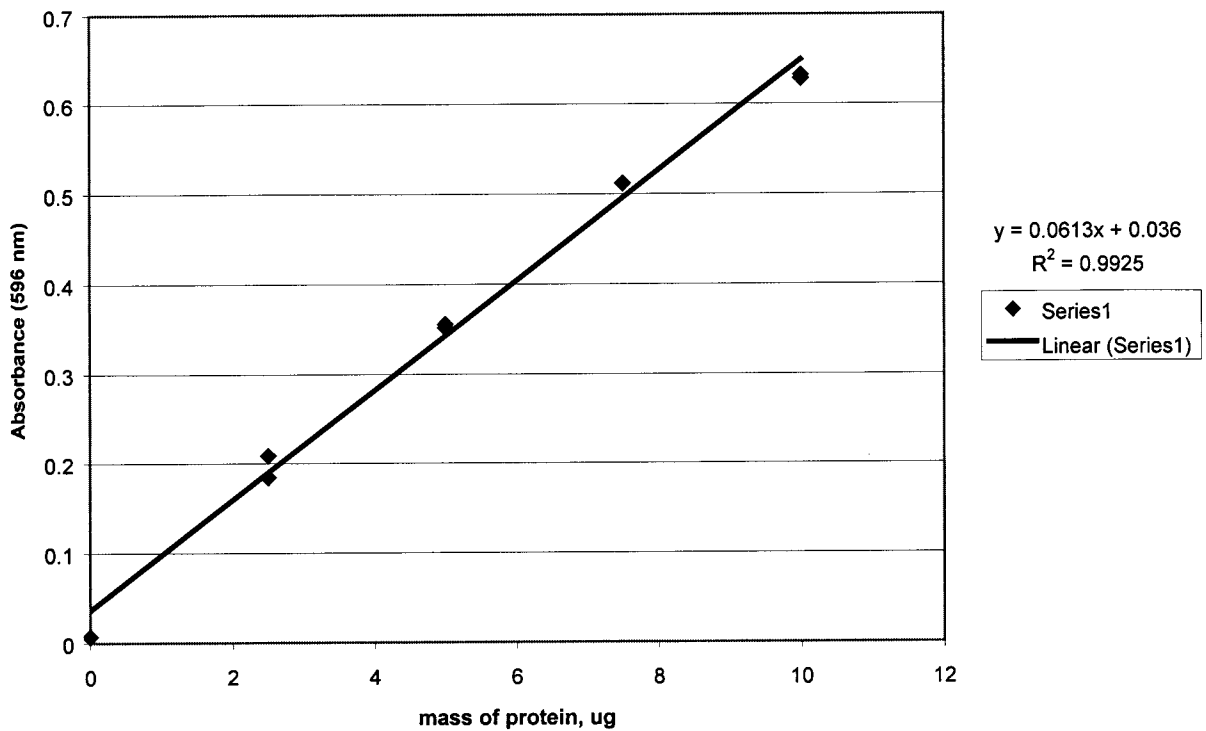


**Figure 18:** Standard Bradford assay curve using 0.5 mg/mL BSA, ODCase concentration is calculated from the equation of the line

### Chapter 3 Inhibition Constants of ODCase Ligands

#### Introduction:

The catalytic mechanism of ODCase involves a proton sensitive step, probably a hydrogen bond to one of the carbonyl oxygens of OMP, and may also include participation of a  $Zn^{+2}$  ion. To study the active site of ODCase, thio-substituted analogues of OMP and UMP were used as inhibitors of yeast ODCase. ODCase was observed to have no catalytic activity towards 2-thioOMP (Figure 20, 1), while its binding activity was reasonably comparable to that of OMP.<sup>14</sup> 4-thioOMP (Figure 20, 2) was found to be a substrate with kinetic parameters similar to those for OMP. In the case of 2-thioOMP, the thiocarbonyl sulfur would be expected to be a weaker base than the carbonyl oxygen, and activity would be expected to decrease in a mechanism involving O2 protonation, but the result was complete disappearance of measurable activity toward 2-thioOMP. We measured the inhibition constants of both 2-thioUMP (Figure 20, 3) and 4-thioUMP (Figure 20, 4) and compared the results obtained to those of UMP, 2-thioOMP, and 4-thioOMP. This study was designed to provide more information on the types of contacts between ODCase and pyrimidine nucleotide ligands. If a decrease in the binding affinities of the thio-analogues compared to that of the substrate was observed then the proton-donating step occurs with the ground state. On the other side, if the Cleland and Kreevoy proposition<sup>18</sup> of a hydrogen bond contact in the transition state was correct, then sulfur substitution might be inconsequential to the binding affinity of thioUMP analogues, since UMP is a ground state inhibitor. Miller *et al.* proved the presence of  $Zn^{+2}$  in yeast ODCase<sup>16</sup>; therefore, if this  $Zn^{+2}$  was involved in catalysis the

sulfur substitution for carbonyl oxygen on the uracil ring of UMP would be expected to lead to a tighter binding affinity.

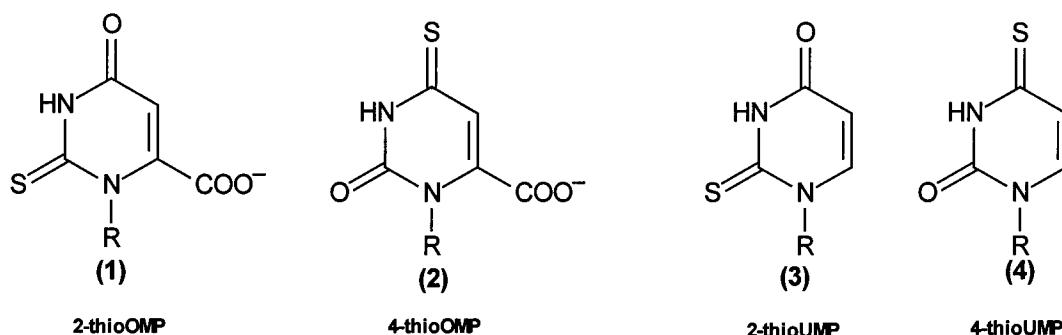


**Figure 20:** Thio-substituted analogues of OMP and UMP used as inhibitors of ODCase.

#### Materials:

4-thioUMP was purchased from Sigma and used without further purification. 2-thioUMP was synthesized enzymatically<sup>24</sup> using 2-thiouracil and 5-phosphorylribose 1-pyrophosphate (PRPP) (Sigma Chemical Co.) and recombinant *Bacillus caldolyticus* uracil phosphoribosyltransferase (UPRTase) produced in *Escherichia coli*<sup>23</sup>. Tryptone was obtained from Fisher Biotech.

#### 2-ThioUMP Synthesis:

*UPRTase preparation:* *E. coli* bacterial strains were provided by Dr. John Neuhard, University of Copenhagen. Strain BM604 carrying plasmid pNK2510, which overproduces UPRTase, was grown in Luria Broth (LB) medium containing 10 g/L tryptone, 5g/L yeast extract, 5g/L NaCl, and adjusted to pH 7.4. 50 mg/mL of ampicillin (Amp) was added to LB medium once at room temperature. 5 mL of LB/Amp medium was inoculated from a selective plate (glucose, Amp, vitamin B<sub>1</sub>, casamino acids, and uracil) and was incubated for 8-9 hr at 37°C. This was then transferred into 25 mL of fresh LB/Amp medium and incubation at 37°C was continued for about 12 hr. The cells

were then harvested by centrifugation at 6000 x g for 10 min and resuspended in 10 mM Tris-HCl buffer at pH 8.6. Crude cellular extracts were obtained by sonic disruptions of the cells using a Branson Sonifer cell disruptor 185 (3 bursts of sonication, 10 sec each), followed by centrifugation at 6000 x g for 10 min to remove cell debris. Protein concentration was then determined by Bradford assay. The UPRTase in this crude extract was used without purification.

*Synthesis of 2-thioUMP:* The synthesis of 2-thioUMP was done according to the methods published by Jensen *et al.*<sup>24</sup> In 5-mL reaction mix (Table 8), 2-thiouracil was converted to 2-thioUMP and progress of the reaction was monitored by silica gel thin layer chromatography (TLC), using a mobile phase of CH<sub>2</sub>Cl<sub>2</sub>:MeOH (19:1 (v/v)) (R<sub>f</sub> 2-thiouracil= 0.3; R<sub>f</sub> 2-thioUMP= 0). Addition of 50% (v/v) ethanol caused the precipitation of the protein that was collected by centrifugation at 6000 x g for 10 min. The supernatant was then evaporated to a final volume of 1 mL, the pH was adjusted to 7.0 with HCl, and water was added to give a final concentration of 1.7 mM as determined from the extinction coefficient,  $\epsilon_{274} = 13,000 \text{ M}^{-1} \text{ cm}^{-1}$ . The product displayed a UV absorbance maximum of 274 nm at pH 7.0, showed a single spot on PEI-cellulose TLC<sup>25</sup>, and was used without further purification.

#### Ionization Constants for Thio-Substituted Analogues:

The absorbances of both 4-thioUMP and 2-thioUMP were measured for the purpose of determining their corresponding pK<sub>a</sub>'s. 4-thioUMP shows a decrease in absorbance at 332 nm with increasing pH while 2-thioUMP shows an increase in absorbance at 240 nm with increasing pH (Table 9). Each nucleotide (20 μM) was dissolved in one of the following buffers at 20 mM: acetate (pH 4.4- 6.2), MOPS (pH-

7.4), Tris-HCl (pH 7.6-8.6), glycine (pH 9.1-10.0), phosphate (pH 11.1-11.9). The plots of absorbance values fit theoretical titration curves (Figure 21) using  $pK_a$  values of 8.6 for 4-thioUMP (Figure 22) and 9.2 for 2-thioUMP (Figure 23). The data used (Table 10) for plotting these graphs were obtained by following equation 2.

$$pH = pK_{\text{theoretical}} + \log \left[ \frac{Abs_{\text{max}} - Abs_{\text{meas}}}{Abs_{\text{meas}} - Abs_{\text{min}}} \right] \quad (\text{Equation 2})$$

where  $Abs_{\text{max}}$  and  $Abs_{\text{min}}$  are the maximum and minimum absorbances and  $Abs_{\text{meas}}$  is the measured absorbance.

#### Enzyme Assays:

Most of the chemical reactions in life are catalyzed by enzymes. These molecules are highly efficient and highly specific; however, their mechanisms of action are often very complicated. Kinetic measurement is one of the most powerful techniques to study enzymatically catalyzed reactions. The rate by which an enzyme facilitates a reaction can be calculated from Michaelis- Menten equation (Equation 3).

$$1/v_0 = (K_m/V_{\text{max}}) 1/[S] + 1/V_{\text{max}} \quad (\text{Equation 3})$$

where “ $v_0$ ” is the initial velocity, “ $K_m$ ” is the substrate concentration at which the reaction velocity is half maximal, [S] is the substrate concentration, and  $V_{\text{max}}$  is the maximum velocity.<sup>23</sup> In the presence of inhibitors, the rate of the enzyme is being decreased. Three different forms of inhibition have been identified which are competitive, uncompetitive, and mixed (noncompetitive). Enzymes as proficient as ODCase were observed to be

sensitive to a class of inhibitors that resemble the transition state. A  $^{14}\text{CO}_2$  displacement assay was used in order to determine the activity of yeast ODCase in the presence of 4-thioUMP and 2-thioUMP, respectively. Reactions (500  $\mu\text{L}$ ) were carried out at  $25^\circ\text{C}$  with 10 mM MOPS, pH 7.0, 0.5-2.0  $\mu\text{M}$   $^{14}\text{C}$ - labeled OMP, and inhibitors at concentrations estimated from preliminary assays carried out by Dr. Jeffrey A. Smiley to be near the  $K_i$  value: [4-thioUMP] = 0, 2.2, or 4.3  $\mu\text{M}$ ; [2-thioUMP] = 0, 31, 61, or 92  $\mu\text{M}$ . ODCase was diluted in 50 mM Tris-HCl, pH 7.4, 10% (v/v) glycerol immediately before assay, so that the amount of activity to convert <30% of substrate to product in 30 sec could be dispensed in 5  $\mu\text{L}$ .  $^{14}\text{C}$ -labelled OMP in the presence of ODCase is converted into UMP and  $^{14}\text{CO}_2$ . The reaction was quenched with 2 M HCl after 30 sec and the liberated gas was collected on a filter paper soaked with base and was then left for 1 hr. After that it was dried in a vacuum oven (Precision Scientific metabolic shaking incubator) for about 30 min and the amount of  $^{14}\text{C}$  was counted in a liquid scintillation counter (Packard Tri-Carb 1900CA Liquid Scintillation Analyzer). In our experiment 1 nmole of product corresponded to 3000 counts per minute (cpm), thus this conversion factor was the key for determining of amount of UMP produced. Table 11 shows the concentrations of OMP and inhibitors used in the experiment.

*4-thioUMP*: The Lineweaver-Burk plot of  $1/v_0$  versus  $1/[\text{S}]$  (Equation 3) at various concentrations of 4-thioUMP:  $[\text{I}] = 0, 2.2, \text{ and } 4.3 \mu\text{M}$ , showed intersecting lines at  $1/V_{\text{max}}$  on the  $1/v_0$  axis (Figure 24). This is diagnostic for competitive inhibition where the inhibitor resembles the substrate to the extent that it binds to the active site of the enzyme. Therefore, a competitive inhibitor reduces the amount of free enzyme available for substrate binding, and this is represented by a general model given in Figure 25.<sup>23</sup>

The  $K_i$  for 4-thioUMP was found to be equal to  $(1.5 \pm 0.5) \times 10^{-6}$  M, determined from the replot of  $K_m$  versus inhibitor concentrations (Figure 26) that followed equation 4.

$$K_{m(\text{app})} = (K_m/K_i)[I] + K_m \quad (\text{Equation 4})$$

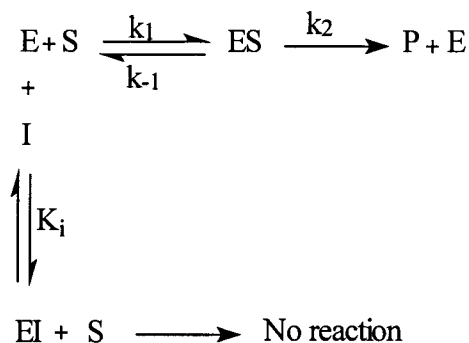


**Figure 25:** The general model for competitive inhibition

*2-thioUMP*: The kinetic plot for inhibition by 2-thioUMP showed intersecting lines to the left of the  $1/v_0$  axis which is an indication of mixed inhibition (Figure 27). The different concentrations of 2-thioUMP at which the rate of catalysis was measured were 0, 31, 61, and 92  $\mu\text{M}$ . In mixed inhibition both the enzyme and the enzyme-substrate complex bind to the inhibitor as illustrated in Figure 28.

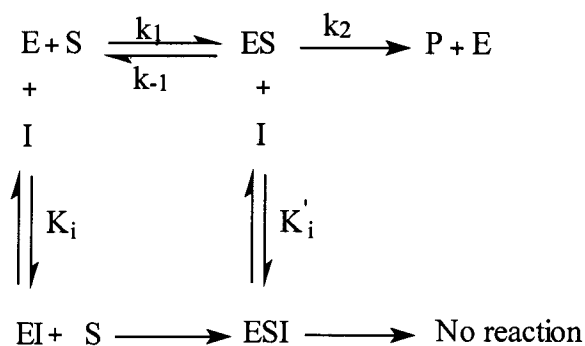


**Figure 28:** The general model for mixed inhibition

Mixed inhibition can act at both low and high substrate concentration. The Lineweaver-Burk plot for mixed inhibition is represented in equation 5,

$$1/v_0 = (\alpha K_m / V_{max}) 1/[S] + \alpha / V_{max} \quad (\text{Equation 5})$$

where  $\alpha = 1 + ([I]/K_i)$ . The  $K_i$  value was determined from replot of the slopes versus each respective inhibitor concentration. The replot was linear (Figure 29) meaning that 2-thioUMP binds to both E and ES, and ESI. Its kinetic mechanism is catalytically inactive and its  $K_i$  was calculated to be equal to  $(43 \pm 7) \times 10^{-6}$  M.

#### Discussion:

The thio-substituted analogues studied by our group had been compared to other ligands: UMP, 2-thioOMP, and 4-thioOMP (Table 12).<sup>21</sup> Both UMP and 4-thioUMP displayed competitive inhibition for ODCase<sup>22</sup>, however the  $K_i$  for 4-thioUMP anion was significantly less than that for UMP suggesting that the active site did not bind UMP as tightly as 4-thioUMP. On the other hand, ODCase showed full activity towards 4-thioOMP while 2-thioOMP had a binding capacity comparable to that of OMP but undetectable substrate activity.<sup>12</sup> In addition to that, 2-thioUMP showed mixed inhibition with an anionic inhibition constant equal to that of UMP. From all of the above clues, we suggested a model for ODCase catalysis in which Lys93 makes a weak, or no, hydrogen bond to O2 of OMP in the ground state. A strong contact between OMP and the enzyme occurs at the transition state level where a low barrier hydrogen bond<sup>17</sup> is formed between Lys 93 on ODCase and O2 on OMP.  $Zn^{+2}$  ion was also suggested to be in contact with the O4 on OMP (Figure 30).



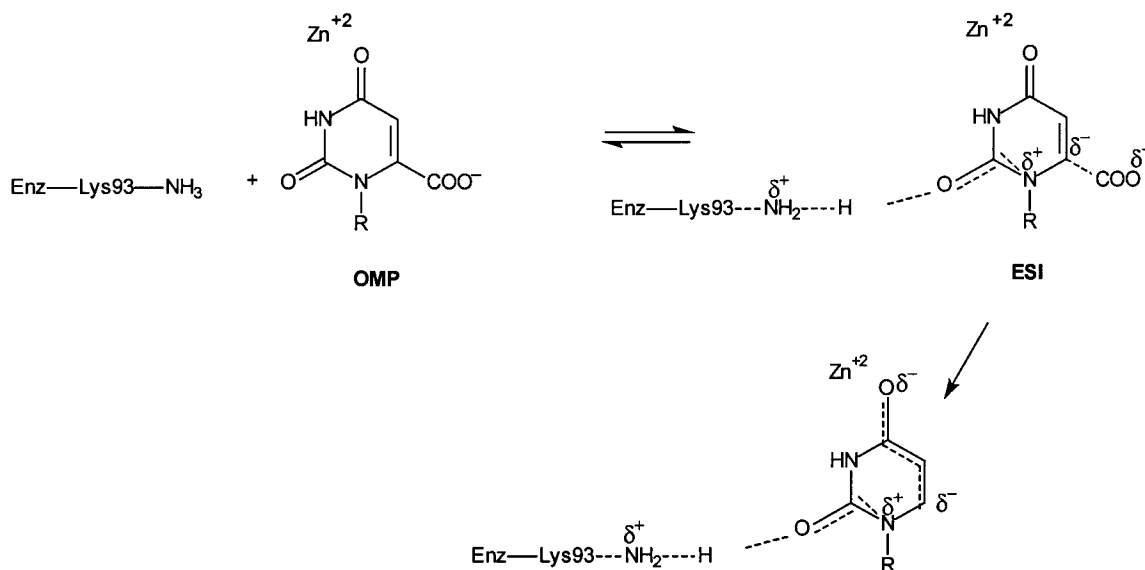


**Figure 30:** Proposed model for decarboxylation of OMP by yeast ODCase

UMP was considered by Levine *et al.*<sup>14</sup> to be a ground state analogue, and thus the hydrogen bond formed between the transition state and the Lys group in the active site did not play a role in the binding of this inhibitor. Both 4-thioUMP and 2-thioUMP were thought of as analogues to the ground state because of their resemblance to UMP and their respective  $K_i$ 's are of a larger value than that of the transition state ( $K_{TS} < 5 \times 10^{-24}$  M). 4-thioUMP was a better inhibitor because of its tighter binding at the fourth position where Zn<sup>+2</sup> made a better contact with sulfur than with oxygen. On the other hand, the sulfur substitution at the second position on UMP did not show a great difference in the values of  $K_i$  since sulfur could not have a stronger attraction to hydrogen than the oxygen. The fact that ODCase showed full activity towards 4-thioOMP could also be explained by our model. 4-thioOMP, a substrate analogue, has the Zn<sup>+2</sup> ion in very tight contact with S4 and a proton shared hydrogen bond at O2. Tight binding of 4-thioOMP allowed for decarboxylation of this analogue. With respect to 2-thioOMP,

the thio substitution on O2 was catastrophic for its activity since the hydrogen bond in the transition state could not be formed.

As a conclusion, our model for the catalytic mechanism of ODCase is still a hypothesis that needs to be proven by a lot of future experiments. Other features of the active site of ODCase as well as the existence of a low barrier hydrogen bond between the enzyme and the transition state remain the subject of further studies.

**Table 8: Reaction mix for synthesis of 2-thioUMP**

Compound	Final concentration	Amount
Tris buffer pH 8.6	100 mM	125 $\mu$ L
MgCl <sub>2</sub>	5 mM	25 $\mu$ L
2-thiouracil	1 mM	500 $\mu$ L
BSA	0.4 mg/mL	500 $\mu$ L
PRPP	1.2 mM	3 mg
H <sub>2</sub> O + UPRtase		4 mL
UPRtase		Volume corresponding to 1 mg = V <sup>a</sup>
H <sub>2</sub> O		4 mL - V

<sup>a</sup>V can be determined from the concentration of UPRtase determined by Bradford assay

**Table 9: Experimental values of 2-thioUMP and 4-thioUMP absorbances obtained upon variation of pH**

2-thioUMP		4-thioUMP	
Experimental pH	Experimental absorbance	Experimental pH	Experimental absorbance
4.37	0.1272	7	0.4477
5.33	0.1146	7.4	0.3925
6.17	0.0984	7.59	0.4241
7.2	0.1435	8.02	0.4074
7.4	0.1714	8.28	0.4148
7.59	0.1483	8.64	0.3554
8.02	0.1456	9.06	0.3362
8.28	0.1468	9.34	0.3179
8.64	0.1646	9.64	0.3231
9.06	0.2647	10.02	0.2716
9.34	0.2579		
9.64	0.3198		
10.02	0.3651		
11.05	0.3684		
11.88	0.3882		

**Table 10: Theoretical data obtained for determination of  $pK_a$ 's for 2-thioUMP and 4-thioUMP**

2-thioUMP		4-thioUMP	
Theoretical pH <sup>a</sup>	Absorbance <sup>b</sup>	Theoretical pH <sup>c</sup>	Absorbance <sup>b</sup>
7.527902	0.145	10.85285	0.281
7.838272	0.15	10.0624	0.286
8.023909	0.155	9.786494	0.291
8.158607	0.16	9.610724	0.296
8.265502	0.165	9.479178	0.301
8.354902	0.17	9.372547	0.306
8.432314	0.175	9.281825	0.311
8.50103	0.18	9.20206	0.316
8.563178	0.185	9.130231	0.321
8.620216	0.19	9.064347	0.326
8.673191	0.195	9.00302	0.331
8.722879	0.2	8.945234	0.336
8.769875	0.205	8.890217	0.341
8.814649	0.21	8.837361	0.346
8.857577	0.215	8.786168	0.351
8.89897	0.22	8.73622	0.356
8.939087	0.225	8.68715	0.361
8.978151	0.23	8.638629	0.366
9.016356	0.235	8.590349	0.371
9.053872	0.24	8.542008	0.376
9.090856	0.245	8.493306	0.381
9.127449	0.25	8.443926	0.386
9.163788	0.255	8.393526	0.391
9.2	0.26	8.341722	0.396
9.236212	0.265	8.288067	0.401
9.272551	0.27	8.232023	0.406
9.309144	0.275	8.172925	0.411
9.346128	0.28	8.109914	0.416
9.383644	0.285	8.041845	0.421
9.421849	0.29	7.967126	0.426
9.460913	0.295	7.883421	0.431
9.50103	0.3	7.787087	0.436
9.542423	0.305	7.671928	0.441
9.585351	0.31	7.52602	0.446
9.630125	0.315	7.321246	0.451
9.677121	0.32	6.956547	0.456
9.726809	0.325		
9.779784	0.33		
9.836822	0.335		
9.89897	0.34		
9.967686	0.345		
10.0451	0.35		
10.1345	0.355		
10.24139	0.36		
10.37609	0.365		
10.56173	0.37		
10.8721	0.375		

<sup>a</sup>For 2-thioUMP:  $\text{pH} = 9.2 + \log [(0.14 - \text{Abs}_{\text{meas}}) / (\text{Abs}_{\text{meas}} - 0.38)]$

<sup>b</sup> $\text{Abs}_{\text{meas}(2)} = \text{Abs}_{\text{meas}(1)} + 0.005$

<sup>c</sup>For 4-thioUMP:  $\text{pH} = 8.6 + \log [(0.46 - \text{Abs}_{\text{meas}}) / (\text{Abs}_{\text{meas}} - 0.28)]$

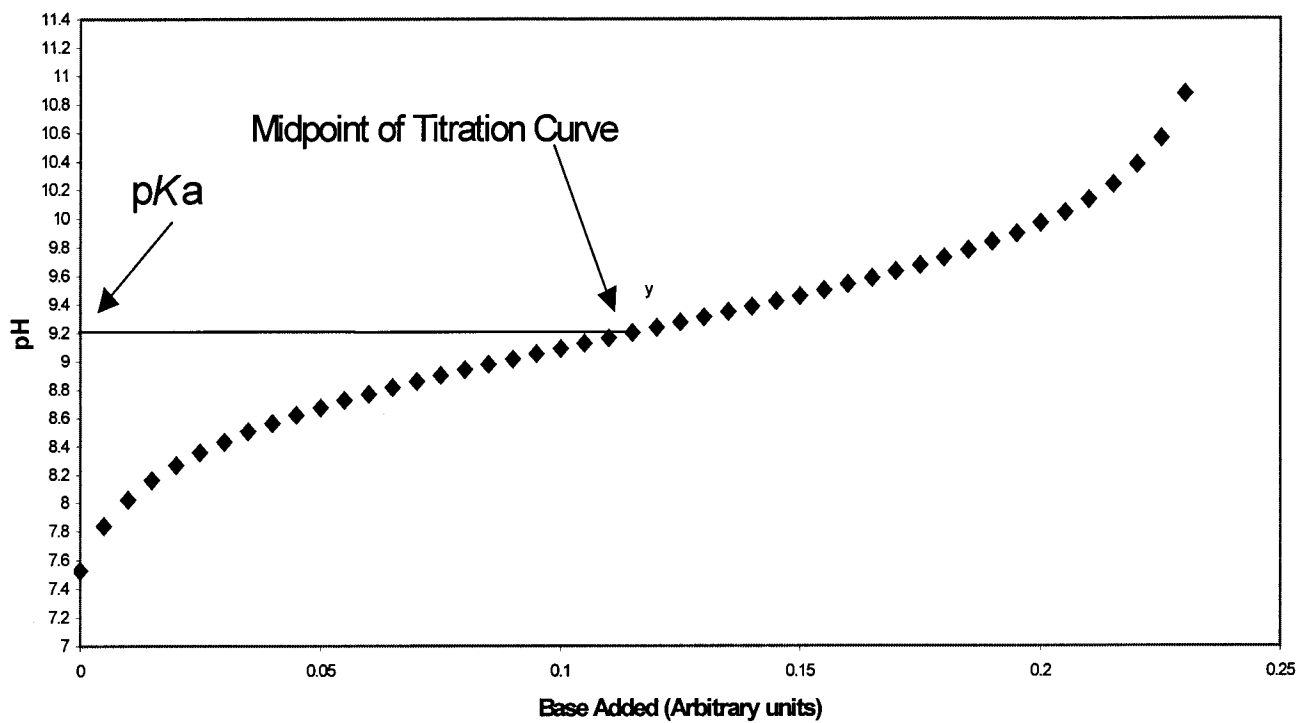
**Table 11: Concentrations of OMP and inhibitors for  $K_i$  determination**

<b>OMP concentration in <math>\mu\text{M}</math></b>	0.5	0.67	1.0	2.0
<b>OMP volume in <math>\mu\text{L}</math></b>	5	6.7	10	20
<b>Mops volume in <math>\mu\text{L}</math></b>	50	50	50	50
<b>ODCase volume in <math>\mu\text{L}</math></b>	5	5	5	5
<b>No inhibitor</b>				
<b>H<sub>2</sub>O volume in <math>\mu\text{L}</math></b>	440	438	435	425
<b>Low inhibitor concentration</b>				
<b>H<sub>2</sub>O volume in <math>\mu\text{L}</math></b>	435	433	430	420
<b>Inhibitor volume in <math>\mu\text{L}</math></b>	5	5	5	5
<b>Medium inhibitor concentration</b>				
<b>H<sub>2</sub>O volume in <math>\mu\text{L}</math></b>	430	428	425	415
<b>Inhibitor volume in <math>\mu\text{L}</math></b>	10	10	10	10
<b>High inhibitor concentration</b>				
<b>H<sub>2</sub>O volume in <math>\mu\text{L}</math></b>	420	418	415	405
<b>Inhibitor volume in <math>\mu\text{L}</math></b>	20	20	20	20

**Table 12: Inhibition constants for UMP and thio-substituted analogues with ODCase**

<b>Inhibitors</b>	<b>Apparent Ki</b>	<b>Ki for anionic form<sup>a</sup></b>
UMP	$(92 \pm 2) \times 10^{-6} \text{ M}^{21}$	$(2.9 \pm 0.1) \times 10^{-7} \text{ M}$
4-thioUMP	$(1.5 \pm 0.5) \times 10^{-6} \text{ M}$	$(0.38 \pm 0.13) \times 10^{-7} \text{ M}$
2-thioUMP	$(43 \pm 7) \times 10^{-6} \text{ M}$	$(2.7 \pm 0.7) \times 10^{-7} \text{ M}$
4-thioOMP		
2-thioOMP		$1.5 \times 10^{-6} \text{ M}^{13}$

<sup>a</sup>Values for Ki of UMP, 2-thioUMP, and 4-thioUMP anions are obtained from Smiley and Saleh<sup>22</sup>, and our calculation were done according to the model of inhibition of Levine *et al.*<sup>14</sup>

**Figure 21: Theoretical titration curve**

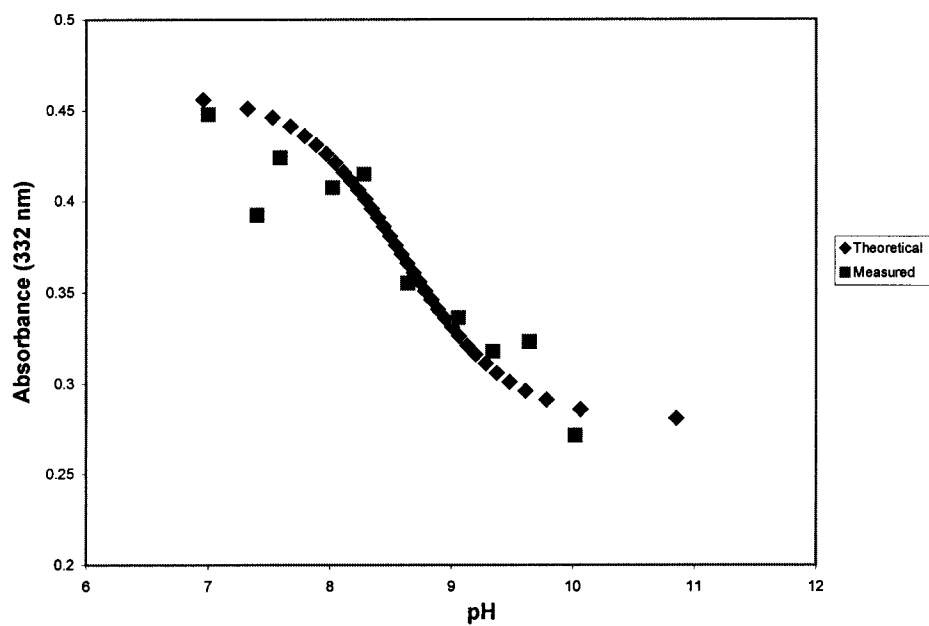


**Figure 22:** Titration curve of 4-thioUMP

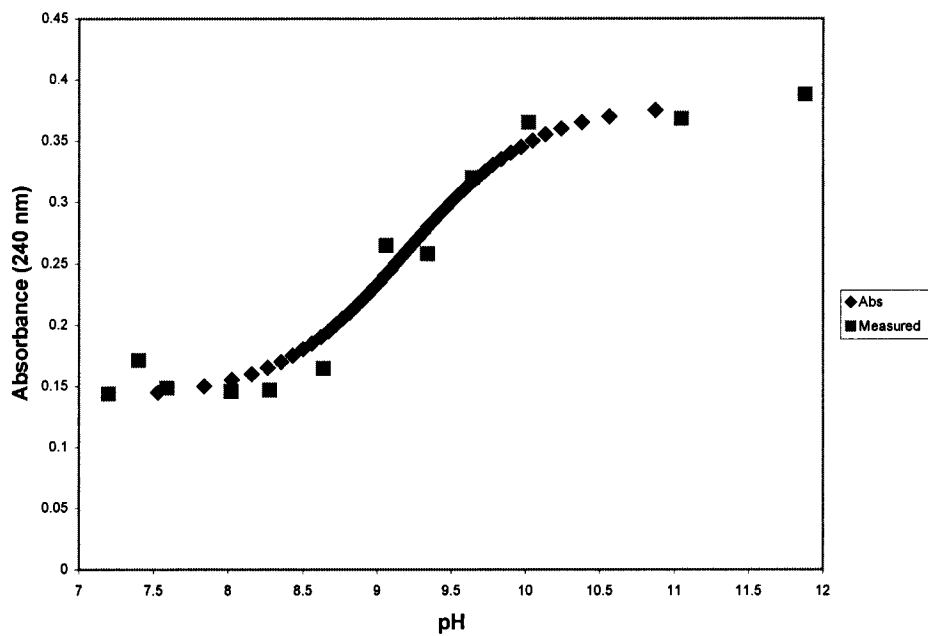


**Figure 23:** Titration curve of 2-thioUMP



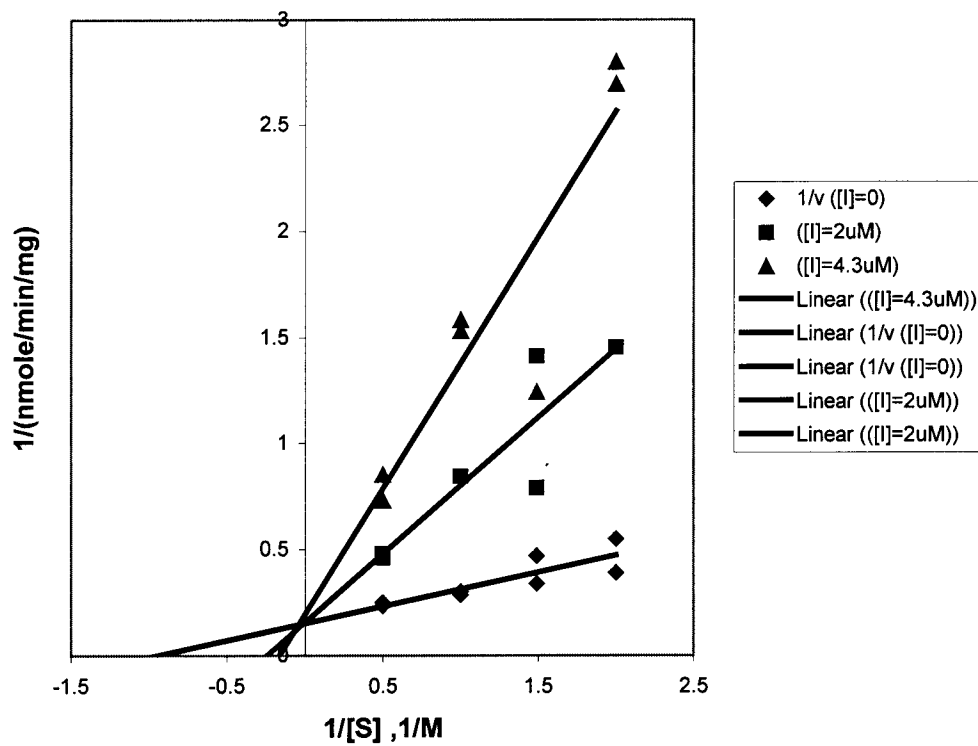


**Figure 24:** Representative kinetic plot for competitive inhibition by 4-thioUMP

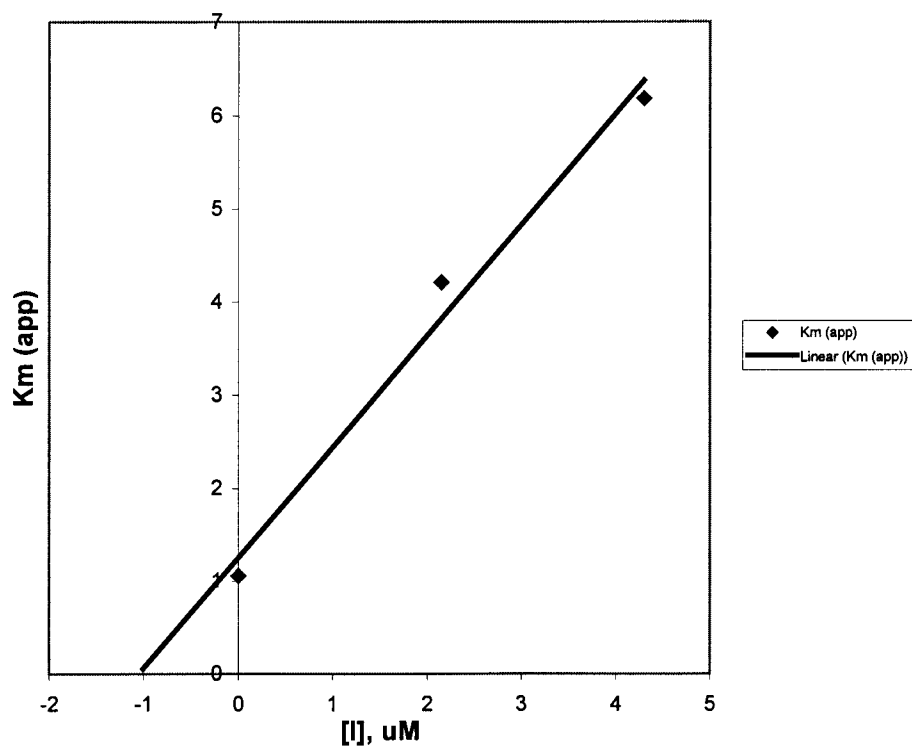


**Figure 26:** Replot of  $K_m$  versus  $[I]$  for  $K_i$  determination of 4-thioUMP

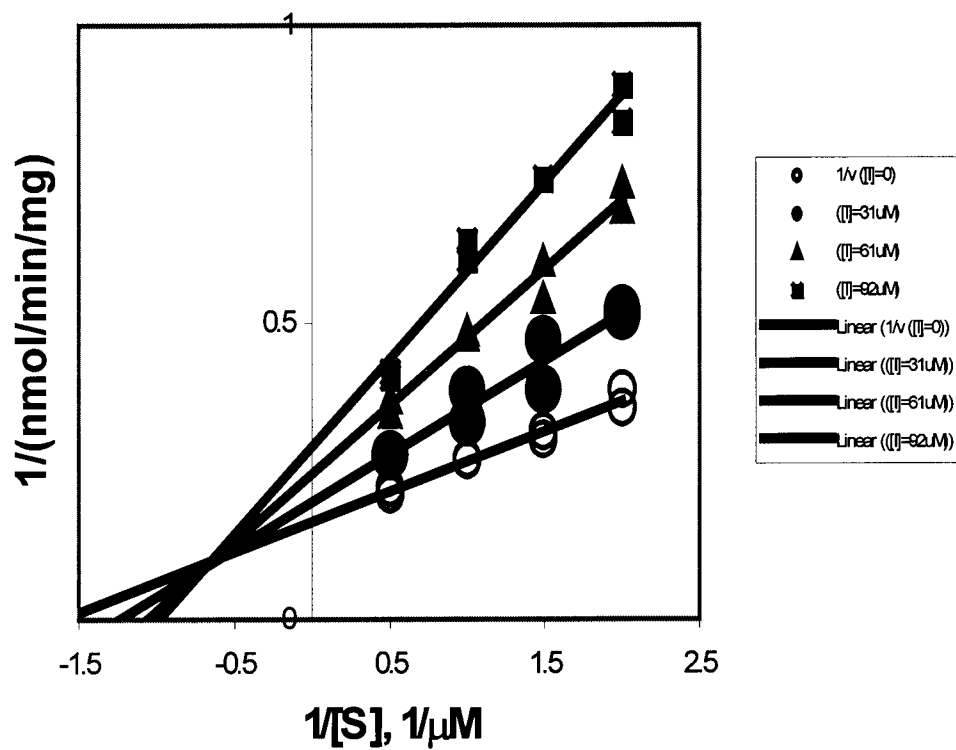


Figure 27: Representative kinetic plot for mixed inhibition by 2-thioUMP

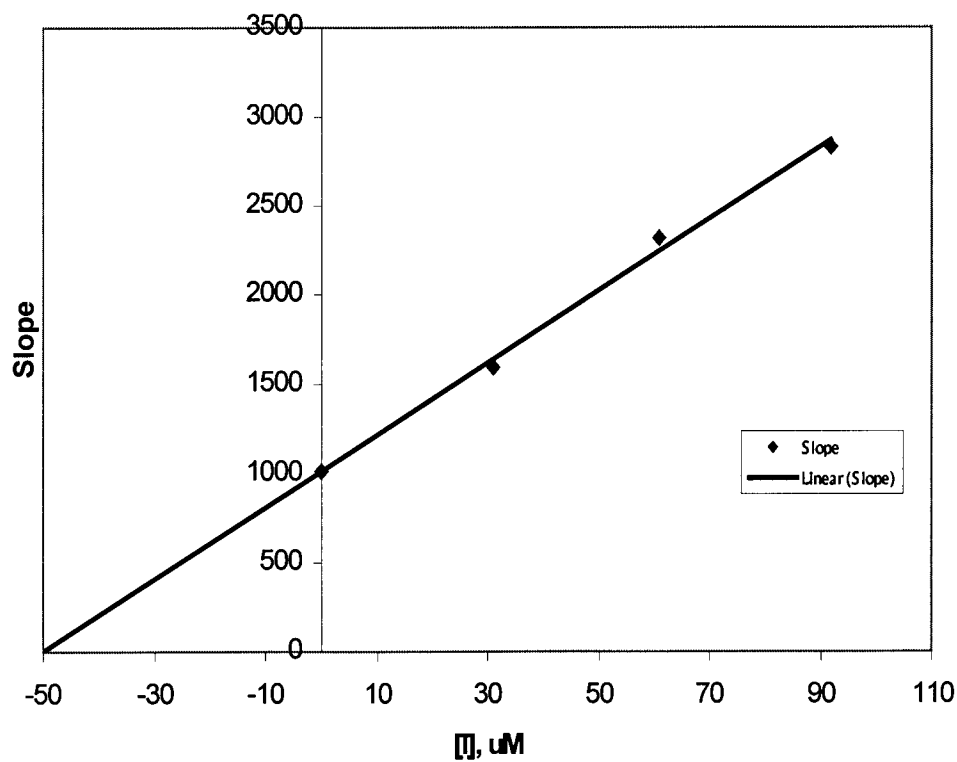


Figure 29: Replot of slope versus  $[I]$  for  $K_i$  determination of 2-thioUMP

## Chapter 4 <sup>1</sup>H NMR Spectral Studies of ODCase Complexes

### Introduction:

The origin of the large catalytic enhancement ( $2 \times 10^{23} \text{ M}$ )<sup>26</sup> of ODCase has been a perplexing issue. Here, we present NMR spectra that might be evidence for the probable existence of a short, strong, or low barrier hydrogen bond (LBHB) between Lys93 and the transition state (Figure 29). Upon binding of barbituric acid ribonucleotide (BMP), an analogue of the transition state, to ODCase, proton NMR detected a deshielded signal at 11.65 ppm. This downfield signal was suspected to be a short, strong (low barrier) hydrogen bond. Another spectrum of an ODCase/UMP complex still showed the 11.65 ppm signal. ODCase does not bind as tightly to UMP as it does to BMP; therefore, we did not expect this result to be obtained. Besides the shift in the proton NMR spectra, a LBHB is expected to show preference for protium over deuterium. As a result, we carried out a fractionation factor experiment with various H<sub>2</sub>O/D<sub>2</sub>O concentrations as an attempt at measuring the exchange rate of this hydrogen bond in ODCase. The results obtained from all the above experiments are to be discussed in detail in the following section.

### Materials:

BMP and UMP were purchased from Sigma. D<sub>2</sub>O was from Cambridge Isotope Laboratories.

### Methods:

Yeast ODCase was purified from strain BJ5424 carrying the plasmid pGU2. The enzyme concentration was determined by Bradford assay. NMR samples for ODCase, ODCase/BMP complex, and ODCase/UMP complex contained 10 mM Tris buffer at

pH 7.4, 5% (v/v) glycerol, 5 mM  $\beta$ -mercaptoethanol, and 10% D<sub>2</sub>O. ODCase concentrations were 9.7mg/mL, 9.7mg/mL, and 16.3 mg/mL respectively for free ODCase, ODCase/BMP, and ODCase/UMP samples. Samples with the transition state analogue (BMP) contained a 1:1 enzyme: ligand molar ratio while that of UMP contained 1:10 enzyme: UMP mole ratio. The general procedure of Loh and Markley<sup>27</sup> was used for determination of the fractionation factors. Five samples with varying amounts of H<sub>2</sub>O/D<sub>2</sub>O (10, 25, 40, 55, and 70% mole fraction D<sub>2</sub>O) were prepared in 50 $\mu$ L solution containing 30 mM Tris buffer at pH 7.4, 10% (v/v) glycerol, 5 mM  $\beta$ -mercaptoethanol. The ODCase/BMP complex was prepared by adding 0.515  $\mu$ mole of each BMP and ODCase to the solution. The mixtures were stirred at 4°C for 24 hr before NMR experiments. According to the Zhao *et al.* procedure<sup>28</sup>, spectra were obtained on a Varian 750 MHz Unity Plus NMR spectrometer, using the 1331 binomial water suppression pulse sequence.

### Results and Discussion:

1-(5'-phosphate- $\beta$ -D-ribofuranosyl) barbituric acid (BMP) is known to be a very good inhibitor of ODCase activity, and it binds about 10<sup>5</sup> times as strongly as the substrate, OMP. The binding of this barbiturate analogue to the enzyme is one of the strongest interactions between a small molecule and a protein that have been measured<sup>17</sup>. BMP has been suggested by Levine *et al.* to be a transition state analogue<sup>14</sup>; therefore, the use of BMP stops the reaction at the intermediate level where it would be possible to study the formation of a hydrogen bond. Our group ran two NMR spectra: one on free ODCase (Figure 31) and the other on the BMP/ODCase complex (Figure 32), both at neutral pH. NMR spectrum of the ODCase/BMP complex showed an 11.5 ppm signal

which probably represents the N3 amide proton of BMP. Signals at 11.2 ppm and farther upfield are essentially the same in both the ODCase/BMP and free ODCase spectra suggesting that they are signals of the free enzyme. The well-defined 12.2 ppm signal in the complex spectrum integrates to two protons and it broadens significantly to 12.0 ppm signal in the free ODCase spectrum probably because of the change in the electronic environment. The 11.65 ppm signal in the ODCase/BMP spectrum was thought to represent the short, strong hydrogen bond since downfield chemical shifts, usually >15 ppm downfield from tetramethylsilane (TMS), are characteristic of this bond. The  $^1\text{H}$  NMR spectrum of ODCase/UMP showed the same signals but in different intensities (Figure 33). This result made us suspicious of our previous conclusion because UMP is a ground state analogue that binds weakly to ODCase ( $K_{i(\text{anionic})} = 9 \times 10^{-12}$ ).<sup>12</sup> Therefore, a LBHB would not be expected to form between UMP and ODCase in the transition state. In addition to that, Miller *et al.* recently reported a crystal structure of the ODCase/BMP complex which showed that Lys93 in yeast ODCase was in contact with C6 (instead of C2) on BMP.<sup>29</sup> This result suggests that a short, strong hydrogen bond might not be behind the large catalytic enhancement of ODCase, or it might not be observable with BMP and further experimentation should be carried to come up with answers.

The fractionation factor experiment was not successful because the 11.65 peaks in the  $^1\text{H}$  NMR spectra of ODCase/BMP with different  $\text{D}_2\text{O}$  concentrations were overlapping and thus their peak areas could not be measured. From this experiment we intended to measure the rate of exchange of the hydrogen bond according to equation 6 where  $\Phi$  is the fractionation factor.<sup>27</sup>

$$\Phi = \frac{[\text{Enz-D}][\text{H}_2\text{O}]}{[\text{Enz-H}][\text{D}_2\text{O}]} \quad (\text{Equation 6})$$



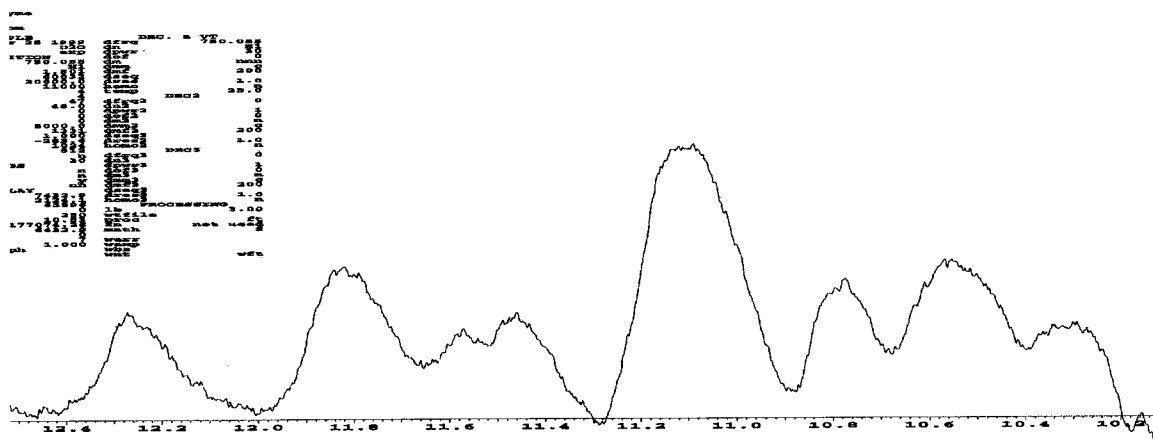


**Figure 33:**  $^1\text{H}$  NMR spectrum of ODCase/UMP in 10 mM Tris buffer at pH7.4, 5% (v/v) glycerol, 5 mM  $\beta$ -mercaptoethanol, and 10% (v/v)  $\text{D}_2\text{O}$ .

## Conclusion

The purification protocol of wild type ODCase yielded ODCase that was free of protein impurities and stable to storage at  $-20^{\circ}\text{C}$  in 20% (v/v) glycerol for 2-3 months. Ninety grams of cells from 4.8 L of cell culture resulted in 1.5 mL of pure ODCase after 9 hr of galactose induction at a concentration of 17-20 mg/mL. Conversely, only partial purification was successful in the case of mutant ODCase (K93C). Protein impurity bands still showed in the 12% SDS-polyacrylamide gels of the fractions obtained from the Affi-Gel Blue and Mono Q anion exchange columns using the Pharmacia FPLC system. The final concentration of the 3 mL fraction of protein sample was 7.32 mg/mL.

The inhibition constants of the thio-substituted analogues were measured using radioactivity-based assays. These analogues were used as active site probes for yeast ODCase. 4-thioUMP was a stronger inhibitor than UMP, while 2-thioUMP had a  $K_i$  virtually the same as that for UMP. Lineweaver Burk plots data used to calculate the inhibition constants showed that 4-thioUMP was a competitive inhibitor, while 2-thioUMP displayed mixed inhibition. These observations led us at that time to propose a model for decarboxylation of OMP by yeast ODCase where the Lys93 side chain shared a short, strong hydrogen bond with O2 of OMP and  $\text{Zn}^{+2}$  ion stabilized the partial negative charge on the O4.

The  $^1\text{H}$  NMR spectra of ODCase/BMP complexes in different  $\text{D}_2\text{O}$  concentrations showed a downfield shift at 11.65 ppm was thought to be formed by a LBHB. However, the results of the  $^1\text{H}$  spectrum of ODCase/UMP as well as the crystal structure of the ODCase/BMP complex cast doubts on the formation of such a bond and implied that our



proposed model needed adjustment. Therefore, future experiments are to be carried out in order to propose a new decarboxylation model for OMP by ODCase.

### References

1. Sigman, D.S. (1992) *The Enzymes* 3<sup>rd</sup> Ed., Vol. 20, pp. 235-269, Academic Press, Inc., San Diego, California.
2. Ingrahm, L.L. (1962) *Biochemical Mechanisms*, pp. 58-68, John Wiley & Sons, Inc., New York, London.
3. Jones, M.E. (1980) *Annu. Rev. Biochem.* **49**, 253-279.
4. McClard, R.W., Black, M.J., Livingstone, L.R., and Jones, M.E. (1980) *Biochemistry* **19**, 4699-47062.
5. Kimsey, H.H., and Kaiser, D. (1992) *J. Biol. Chem.* **267**, 819-824.
6. Bell, J.B., and Jones, M.E. (1991) *J. Biol. Chem.* **266**, 12662-12667.
7. Lue, N.F., Chasman, D.I., Buchman, A.R., and Kornberg, R.D. (1987) *Mol. Cell. Biol.* **7**, 3446-3451.
8. Lee, J.K., and Houk, K.N. (1997) *Science* **276**, 942-945.
9. Wagner, R., and Philipsborn, W.V. (1970) *Helv. Chim. Acta* **53**, 299.
10. Beak, P., and Siegel, B. (1976) *J. Am. Chem. Soc.* **98**, 3601-3606.
11. Smiley, J.A., Paneth, P., O'Leary, M.H., Bell, J.B., and Jones, M.E. (1991) *Biochemistry* **30**, 6216-6223.
12. Shostak, K., and Jones, M.E. (1992) *Biochemistry* **31**, 12155-12161.
13. Silverman, R.B., and Groziak, M.P. (1982) *J. Am. Chem. Soc.*, **104**, 6436-6439.
14. Levine, H.L., Brody, R.S., and Westheimer, F.H. (1980) *Biochemistry* **19**, 4699-47062.
15. Acheson, S.A., Bell, J.B., Jones, M.E., and Wolfenden, R. (1990) *Biochemistry* **29**, 3198-3202.

16. Miller, B.G., Traut, T.W., and Wolfenden, R. (1998) *J. Am. Chem. Soc.* **120**, 2666-2667.
17. Smiley, J.A., and Jones, M.E. (1992) *Biochemistry* **31**, 12162-12168.
18. Cleland, W.W., and Kreevoy, M.M. (1994) *Science* **264**, 1887-1890.
19. Cleland, W.W., Frey, P.A., and Gerlt, J.A. (1998) *J. Biol. Chem.* **273**, 25529-25532.
20. Gerlt, J.A., Kreevoy, M.M., Cleland, W.W., and Frey, P.A. (1997) *Chemistry & Biology* **4**, 259-s267.
21. Smiley, J.A., and Saleh, L. (1999) *Bioorganic Chemistry* **27**, 297-306.
22. Robyt, J., White, B. (1990) *Biochemical Techniques: Theory and Practice*, pp. 73-128, Waveland Press, Inc., Illinois.
23. Voet, D., and Voet, J.G. (1995). *Biochemistry* 2<sup>nd</sup> Ed., pp. 78-95, John Wiley & Sons, Inc., Somerset, N.J.
24. Jensen, H.K., Mikkelsen, N., and Neuhard, J. (1997) *Protein Expression and Purification* **10**, 356-364.
25. Payne, R., and Traut, T.W. (1982) *Anal. Biochem* **121**, 49-54.
26. Radzicka, A., and Wolfenden, R. (1995) *Science* **267**, 90-93.
27. Loh, S.N., and Markley, J.L. (1994) *Biochemistry* **33**, 1029-1036.
28. Zhao, Q., Abeygunawardana, C., Talalay, P., and Mildvan, A.S. (1996) *Biochemistry* **93**, 8220-8224.
29. Personal Contacts: Miller, B.G., Traut, T.W., and Wolfenden, R. (1999), University of North Carolina, Chapel Hill.